Transdiagnostic dimensions of psychopathology explain individuals' unique deviations from normative neurodevelopment in brain structure

Linden Parkes PhD[1], Tyler M. Moore PhD[2,3], Monica E. Calkins PhD[2,3], Philip A. Cook PhD[6], Matthew Cieslak PhD[2,3,4], David R. Roalf PhD[2,3], Daniel H. Wolf MD PhD[2,3,4], Ruben C. Gur PhD[2,3,5,6], Raquel E. Gur MD PhD[2,3,5,6], Theodore D. Satterthwaite MD*[2,3,4], Danielle S. Bassett PhD*†[1,2,5,7,8,9]

[1]Department of Bioengineering, School of Engineering & Applied Science, University of Pennsylvania, Philadelphia, PA, 19104 USA.
[2]Department of Psychiatry, Perelman School of Medicine, University of Pennsylvania, Philadelphia, PA 19104, USA.
[3]Lifespan Brain Institute, University of Pennsylvania & Children's Hospital of Philadelphia, Philadelphia, USA
[4] Center for Biomedical Image Computing and Analytics, Perelman School of Medicine, University of Pennsylvania, Philadelphia, PA 19104 USA.
[5]Department of Neurology, Perelman School of Medicine, Philadelphia, PA 19104 USA.
[6]Department of Radiology, Perelman School of Medicine, Philadelphia, PA 19104 USA.
[7]Department of Electrical & Systems Engineering, School of Engineering & Applied Science, University of Pennsylvania, Philadelphia, PA, 19104 USA.
[8]Department of Physics & Astronomy, College of Arts & Sciences, University of Pennsylvania, Philadelphia, PA, 19104 USA.
[9]Santa Fe Institute, Santa Fe, NM 87501 USA
†To whom correspondence should be addressed: dsb@seas.upenn.edu
*Authors contributed equally

Corresponding author: Danielle S. Bassett, dsb@seas.upenn.edu, Suite 240 Skirkanich Hall, 210 Sth 33rd St, Philadelphia, PA 19104-6321, USA

Running title: Psychopathology and normative neurodevelopment

Keywords: Dimensional psychopathology, normative modeling, normative neurodevelopment, structural MRI

Manuscript word count: 3,825

ABSTRACT

Background: Psychopathology is rooted in neurodevelopment. However, clinical and biological heterogeneity, and a focus on case-control approaches, have made it difficult to link specific forms of psychopathology to abnormalities of neurodevelopment.

Methods: We used clinical symptom data and T1-weighted MRI data in 1,393 youths aged 8 to 22 years from the Philadelphia Neurodevelopmental Cohort. Normative neurodevelopment of cortical volume and thickness was estimated using Gaussian Process Regression in 410 healthy individuals. Deviations from normative neurodevelopment were estimated in the remaining 983 individuals who reported lifetime psychopathology. Next, we distilled 117 clinical symptom measures into six orthogonal psychopathology dimensions: overall psychopathology, anxious-misery, externalizing disorders, fear, positive psychotic symptoms, and negative psychotic symptoms. Psychopathology dimensions were correlated with regional deviations from normative neurodevelopment. We also performed conventional case-control comparisons of deviations in a group of individuals with depression and a group with attention-deficit hyperactivity disorder (ADHD).

Results: Psychopathology dimensions were associated with spatially varied patterns of deviations from normative neurodevelopment. In particular, greater overall psychopathology was associated with neurodevelopmentally advanced volume reductions in ventromedial prefrontal, inferior temporal, dorsal anterior cingulate, and insula cortices, all regions consistently implicated in a range of putatively distinct disorders. Furthermore, case-control comparisons of deviations revealed spatially overlapping group-level effects for depression and ADHD, which diminished when controlling for overall psychopathology.

Conclusions: Case-control comparisons are confounded by overall psychopathology, rendering them unlikely to yield meaningful biomarkers. Instead, the neural underpinnings of psychopathology may be better elucidated by

integrating dimensional models of psychopathology with models of normative neurodevelopment.

INTRODUCTION

Throughout childhood, adolescence, and young adulthood the brain undergoes major structural changes that facilitate the emergence of complex behavior and cognition (1,2). Mental disorders often surface during this period (3) and are increasingly understood as resulting from disruptions to normative brain maturation (4,5). While maturational changes are stereotyped at the population level, substantial individual variation is also reported (2). The extent to which this individual variation in neurodevelopment may explain psychopathology remains unclear.

Linking abnormalities in neurodevelopment to psychopathology has been limited by several challenges. First, diagnostic nosologies assign individuals with distinct symptom profiles to the same clinical diagnosis, yielding disorder groups with highly heterogenous clinical presentation (6). Second, comorbidity among disorders is high (7–9), rendering it difficult to detect the neural correlates of specific disorders. Third, much of the extant literature has adopted case-control designs that reveal only abnormalities associated with the 'average' patient, ignoring the dimensional nature of psychopathology (10). Research linking individuals' neurodevelopmental alterations with distinct dimensions of psychopathology relevant to multiple disorders is a critical step toward developing diagnostic biomarkers for mental health (11–15).

A promising approach entails examining dimensions of symptoms that cut across diagnostic categories (16). The *p-factor* hypothesis (10,17–19) posits that psychopathology symptoms cluster into latent dimensions including a general factor (known as *p* or 'overall psychopathology'), which underpins individuals' tendency to develop all forms of psychopathology, alongside multiple dimensions that describe specific types of psychopathology. This dimensional scoring can be accomplished with a bifactor model (20), which yields specific factors (e.g., externalizing, psychosis) that are orthogonal to the general factor and to each other. Previous research has revealed that such psychopathology dimensions relate to differences in brain structure (19,21–24). However, whether these psychopathology dimensions help elucidate abnormal neurodevelopment remains unclear.

Here, we evaluated whether dimensions of psychopathology relate to individual differences in neurodevelopment. Using a bifactor model, we modeled overall psychopathology and five specific factors, corresponding to mood and anxiety symptoms, externalizing behavior, fear, positive psychosis symptoms, and negative psychosis symptoms (21,25,26). We integrated these psychopathology dimensions with T1-weighted neuroimaging data using a contemporary machine learning technique known as *normative modeling* (27). Here, a normative model is a statistical model that finds the relationship between age and any brain feature, as well as the variation in this relationship expected in a group of healthy individuals. Then, the brains of individuals who experience psychopathology can be understood with respect to this normative model, allowing identification of regional deviations from normative neurodevelopment for each individual (28–30).

The above framework is applicable to any brain feature that changes reliably with age. Here, we focused on cortical gray matter, indexed via *cortical volume* and *cortical thickness,* which is known to undergo plastic maturation in youth, including showing a robust global decrease from childhood to adulthood, reflecting cortical myelination and potentially synaptic pruning (31–34). Prior work has shown widespread non-uniform reductions in gray matter across major depressive disorder (35,36), schizophrenia (37), bipolar disorder (38), and anxiety disorders (39). Across these disorders, overlapping reductions were particularly found in ventromedial prefrontal / medial orbitofrontal cortex (vmPFC/mOFC), inferior temporal, dorsal anterior cingulate (daCC), and insula cortices (39,40).

We tested the primary hypothesis that dimensions of psychopathology are associated with unique deviations from normative neurodevelopment. Specifically, we examined the relationship between regional deviations from normative neurodevelopment and inter-individual differences in dimensions of psychopathology. We expected that overall psychopathology would explain the common abnormalities observed in case-control literature (39,40), and predicted that greater overall psychopathology would be predominantly associated with greater negative deviations (i.e., accelerated reductions with respect to the normative age pattern) in cortical gray matter in the vmPFC/mOFC, inferior temporal, daCC, and insula cortices. Drawing on our previous work (21), we also

expected the fear dimension to be associated with accelerated reductions in the anterior and posterior cingulate, insula, and temporal-parietal junction.

Our secondary aim was to assess the extent to which overall psychopathology explained the overlap between group-level differences observed for traditional case-control analyses. Specifically, we examined group-level deviations from the normative model in two samples, one with depression and another with attention-deficit hyperactivity disorder (ADHD). We expected that both groups would show correlated patterns of average deviations from normative neurodevelopment. Critically, we hypothesized that the correlation between patterns of average deviations would diminish when overall psychopathology was controlled for in our sample, indicating a lack of sensitivity of a case-control approach to detect disorder-specific biomarkers.

MATERIALS AND METHODS

Figure 1 displays the workflow of our analyses. All analytic code can be found at: https://github.com/lindenmp/NormativeNeuroDev_CrossSec_T1

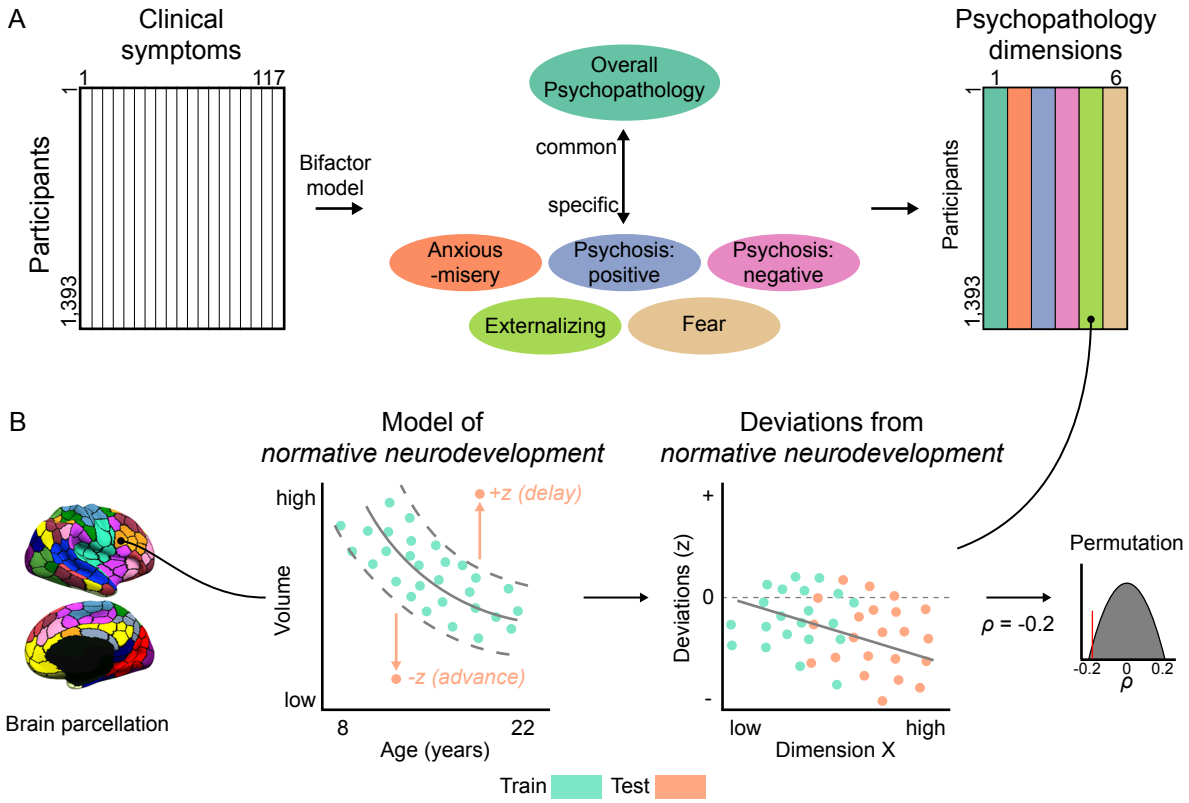

Figure 1. **Schematic illustration of analyses conducted in the current study**. **A**, 117 items from psychopathology symptom rating scales were distilled into six orthogonal psychopathology phenotypes using bifactor analysis. **B**, Individuals were assigned to *train* ( ) and *test* ( ) subsets based on the absence or presence of psychopathology, respectively. Normative models learned the relationship between age (and sex) and brain features using the *train* subset, and deviations from this normative pattern were estimated for the *test* subset. Deviations in the *train* subset were estimated via 10-fold cross-validation. Correlations between psychopathology phenotypes and deviations were calculated, and *p*-values were assigned by a non-parametric permutation test.

Participants

Participants included 1,601 individuals from the Philadelphia Neurodevelopmental Cohort (41), a large community-based study of brain development in youths aged 8 to 22 years. We studied a subset of 1,393 participants, including individuals who were medically healthy and passed stringent neuroimaging quality control (see Supplementary Methods).

Psychopathology phenotyping

Details of the dimensional psychopathology model have been published elsewhere (25,42) (see Supplementary Methods). Briefly, we used confirmatory bifactor analysis to quantify six orthogonal dimensions of psychopathology, including an overall psychopathology factor common to all symptoms measured herein, and five specific factors: anxious-misery, psychosis-positive, psychosis-negative, externalizing behaviors, and fear (Figure 1A; see Table S2 for factor loadings). Note, this model expands on our previous model (21,26,43) by splitting psychosis into positive and negative dimensions (44).

Normative modeling

For details on image acquisition, processing, quality control, and derivation of brain features see Supplementary Methods. Briefly, regional cortical thickness and volume were extracted for each of 400 brain regions defined by the Schaefer atlas (45). Next, we built normative models to predict regional cortical thickness and volume (Figure 1B). In order to estimate *normative* neurodevelopmental trajectories, we split our sample of 1,393 participants into two groups based on the presence or absence of psychiatric history. A total of 410 individuals reported no clinically significant symptoms on any disorder examined and are hereafter designated as our normative *training* subset. The remaining 983 individuals who reported experiencing psychopathology are hereafter referred to as the *testing* subset. Next, for each brain feature and region (*j*), we used Gaussian Process Regression (GPR) to predict regional brain feature values from age and sex using the training subset (see Marquand *et al.* (27) and https://github.com/amarquand/PCNtoolkit for details). A key advantage of this approach is that in addition to fitting potentially non-linear predictions of a brain feature, it also provides regional estimates of the expected variation in the relationship between age and brain features (normative variance) as well as estimates of uncertainty in this variance. Both normative variance and uncertainty are learned from the training subset. Then, for each participant (*i*) in the test subset, we generated the predicted brain feature ($\hat{y}_{ij}$) and combined it with the true value of the brain feature (y_{ij}), the predictive uncertainty (σ_{ij}), and the normative

variance (σ_{nj}) to create a *z*-score that quantified deviation from normative neurodevelopment (27):

$$z_{ij} = \frac{y_{ij} - \hat{y}_{ij}}{\sqrt{\sigma_{ij}^2 + \sigma_{nj}^2}}.$$

This normative model stands in contrast to alternative approaches, such as so-called brain age models (46), that typically estimate deviations from linear relationships and that do not incorporate estimates of normative variance and uncertainty into the derivation of deviations (15). Mass univariate application of the normative model to regional thickness and volume yielded a 983 × 800 *z*-score deviation matrix for the testing subset. Next, we used 10-fold cross-validation to also generate deviations in the training subset. The 410 individuals in the training subset were split into 10 folds, wherein 90% of the subset were used to re-train the GPR in order to generate z-score deviations in the remaining 10%. Together this yielded a 1,393 × 800 *z*-score deviation matrix, $\boldsymbol{F_z}$.

Interpreting deviations from normative models

We were interested in interpreting the extent to which deviations in $\boldsymbol{F_z}$ represented neurodevelopmental delay or advance with respect to the normative trajectory. This information is encoded in the sign of the *z*-score. However, whether a positive or negative *z*-score corresponds to delay or advance is determined by the underlying age effect. If the normative trajectory was characterized by a decrease in the brain feature with advancing age, then positive deviations could be considered a delay in this decrease, and negative deviations could be considered an advance of this decline (e.g., Figure 1B). In contrast, if the normative trajectory was characterized by an increase in a brain feature as a function of increasing age, then the opposite would be the case. Note, we do not interpret delay or advance as inherently 'bad' or 'good'. Instead, delay and advance are used to lend interpretation to the z-scores with respect to what is normative for our healthy training subset.

Correlations between psychopathology dimensions and brain features

To test our primary hypothesis that each psychopathology dimension would be associated with unique patterns of abnormal neurodevelopment, Spearman rank correlations were calculated between each psychopathology dimension from the *p-factor* model and each of the columns in $\boldsymbol{F_z}$, controlling for age and sex. Significance was assigned using permutation testing and multiple comparisons were rigorously corrected across regions and psychopathology dimensions (2,400 tests) using the Benjamini and Hochberg False Discovery Rate (FDR, q = 0.05) procedure (47) (see Supplementary Methods). Next, to examine whether different psychopathology dimensions were associated with deviations from normative neurodevelopment in specific brain systems, we summarized our results across 17 canonical systems of the brain (48). For each brain system, we visualized spatial extent by calculating the proportion of regions that showed significant correlations to a given dimension separately for positive and negative relationships. This approach visualized the spatial extent to which different brain systems were implicated by different dimensions of psychopathology.

Case-control comparisons of deviations from normative neurodevelopment

To test our assertion that *p-factor* models of psychopathology provide more precise insights into neurodevelopmental structural brain abnormalities, we selected a subsample of our test subset with clinically significant depression (*N* = 144, *Mean age* = 17.62±2.28 years, 33% males) and a subsample with clinically significant ADHD (*N* = 188, *Mean age* = 13.62±3.10, 62% males), two disorders with distinct clinical presentations, and performed case-control analyses. In each group, we excluded participants with comorbid depression and ADHD. We estimated group-level deviations from normative neurodevelopment by calculating regional Cohen's *D* values comparing the deviations from each group with deviations from the training subset, controlling for age and sex. Then, to assess correspondence between group-level effects for depression and ADHD, we estimated the spatial (Pearson's) correlation between regional Cohen's *D* values. Finally, to examine the extent to which regional variation in Cohen's *D* values was explained by overall

psychopathology, we re-estimated the spatial correlation between regional Cohen's *D* values after controlling for overall psychopathology.

RESULTS

Participants and age effects

Figure 2A-B display sample demographics and psychopathology scores as a function of the *training* and *testing* subsets. For both males (Figure 2C) and females (Figure 2D), the normative model revealed that greater age was associated with whole brain decreases in cortical thickness and volume. Thus, for the purposes of subsequent analyses of the psychopathology dimensions, positive correlations were interpreted as greater psychopathology scores being associated with neurodevelopmental delay (greater positive *z*-scores) and negative correlations were interpreted as greater psychopathology scores being associated with neurodevelopmental advance (greater negative *z*-scores).

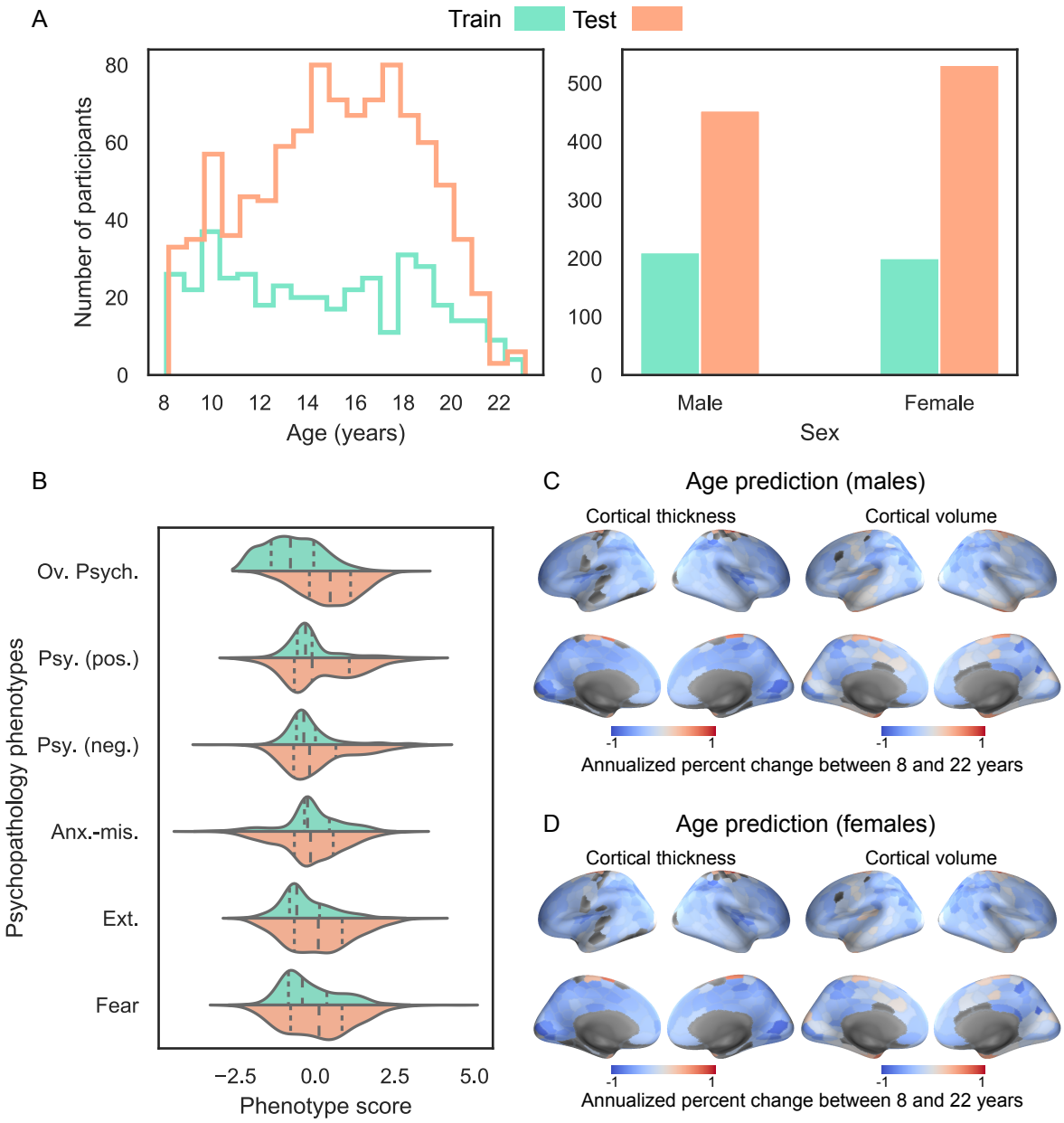

Figure 2. **Participant demographics and psychopathology phenotypes as a function of the train and test split as well as age trajectories of brain features learned by the normative model. A**, Participant demographics for 410 individuals who reported no clinical symptoms on any disorder examined (*train*) and 983 individuals who did report experiencing psychopathology (*test*). **B**, Scores on psychopathology phenotypes as a function of *train* and *test*. Vertical long-dash lines represent the median of each distribution and vertical short-dash lines represent the upper and lower quartiles. **C**, Predicted change (expressed as annualized percent change) across thickness and volume features for *males* between ages 8 and 22 years from the normative model trained on the *train* subset. **D**, Predicted change across thickness and volume for *females* between ages 8 and 22 years from the normative model trained on the *train* subset. Ov. Psych. = overall psychopathology, Psy. (pos.) = psychosis-positive, Psy. (neg.) = psychosis-negative, Anx.-mis. = anxious-misery, Ext. = externalizing behavior.

Psychopathology dimensions explain regional deviations from normative neurodevelopment

To address our primary hypothesis, we examined the relationship between psychopathology dimensions and deviations from normative neurodevelopment. We found that cortical volume yielded more significant effects than cortical thickness. Indeed, only the fear dimension showed significant correlations in >5% of brain regions for thickness. Overall psychopathology, psychosis-positive, and externalizing yielded significant correlations with thickness in <5% of regions, and psychosis-negative and anxious-misery showed no significant correlations.

Concerning cortical volume, in support of our hypothesis, we found that greater overall psychopathology was associated with advanced volume reductions in the vmPFC/mOFC, inferior temporal, daCC, and insula cortices (Figure 3A). Notably, advanced volume reductions in the inferior temporal cortex was observed to a greater extent for psychosis-positive (Figure 3B) compared to psychosis-negative (Figure 3C) and anxious-misery (Figure 3D), suggesting that positive psychotic symptoms accounted for abnormal neurodevelopment in the inferior temporal cortex beyond that accounted for by overall psychopathology. Second, consistent with prior work (21), greater scores on the fear dimension were associated with developmentally advanced volume reductions in the insula cortex as well as many other regions.

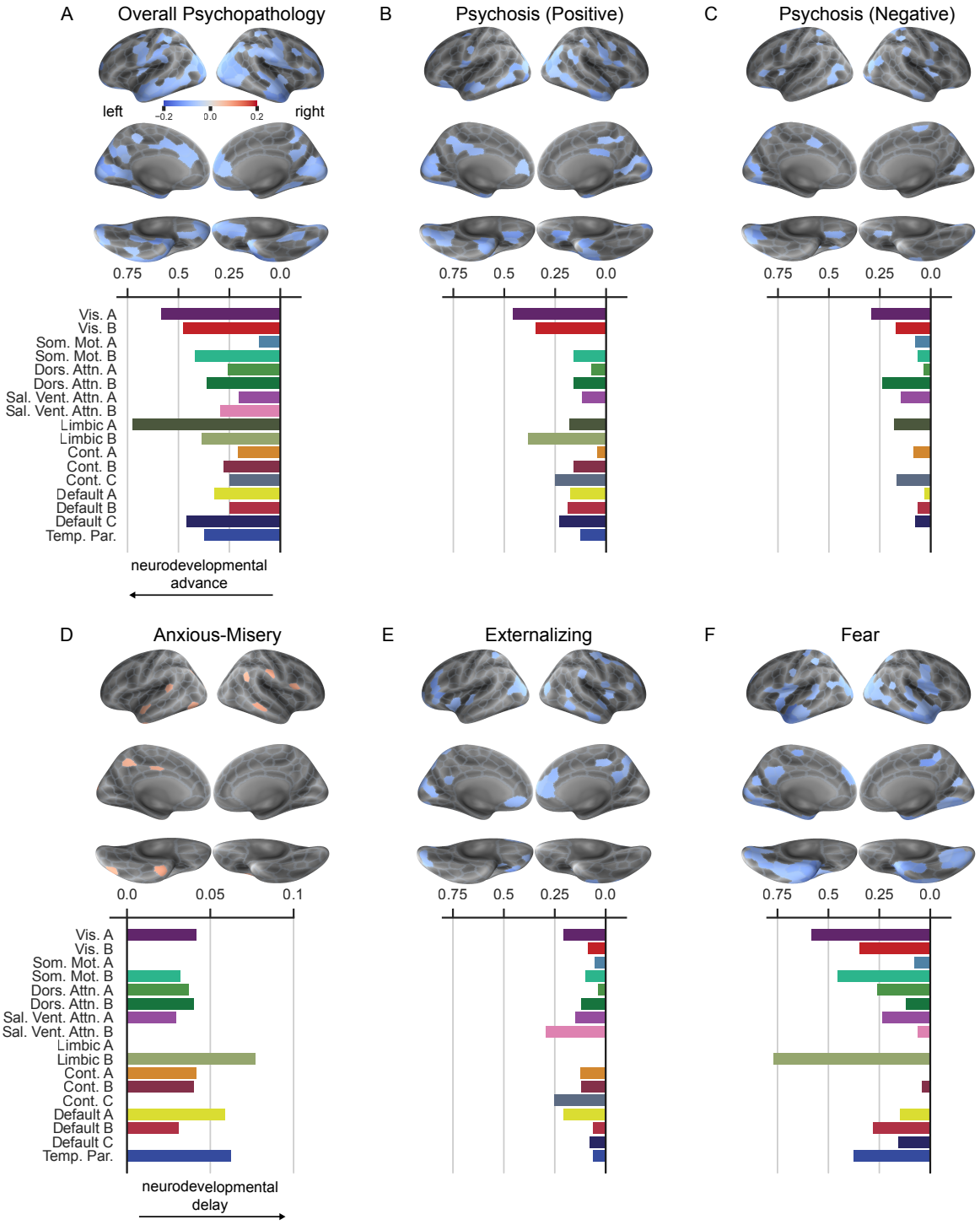

Figure 3. **The relationship between dimensions of psychopathology and deviations from normative neurodevelopment for *cortical volume* varies over brain systems. A-F**, Significant ρ correlations between the dimension of psychopathology and deviations from the normative model. For positive correlations, greater scores on the psychopathology dimension are associated with greater neurodevelopmental delay. For negative correlations, greater scores on the psychopathology dimension are associated with greater neurodevelopmental advance. The proportion of significant signed effects within each of 17 Yeo brain systems are shown in the lower panel of each subplot. Bars emerging from the left of 0 represent the negative correlations and bars emerging from the right of 0 represent the positive correlations. *Note*: Only regions where standardized mean squared error was < 1 are presented.

Summarizing findings at the system level, our results demonstrate that while most psychopathology dimensions (except anxious-misery) were associated with neurodevelopmentally advanced volume reductions, the extent to which different systems were implicated varied substantially. For example, the effects of overall psychopathology (Figure 3A) most broadly implicated the Limbic A system, whereas fear (Figure 3F) most broadly implicated the Limbic B system. The psychosis-positive dimension implicated the default mode and control systems (Figure 3B) more broadly than did the psychosis-negative (Figure 3C) dimension. For the externalizing dimension (Figure 3E) we found a gradient of increasing number of effects going from dorsal attention to ventral attention systems whereas the opposite was observed for fear. On the other hand, a surprising consistency in our results was that overall psychopathology, psychosis-positive, psychosis-negative, and fear all showed relatively widespread effects in the visual system. Concerning the results for cortical thickness, similar to volume, greater scores on each of the psychopathology dimensions was associated with advanced reductions (Figure 4) that varied by brain system, albeit to a lesser extent.

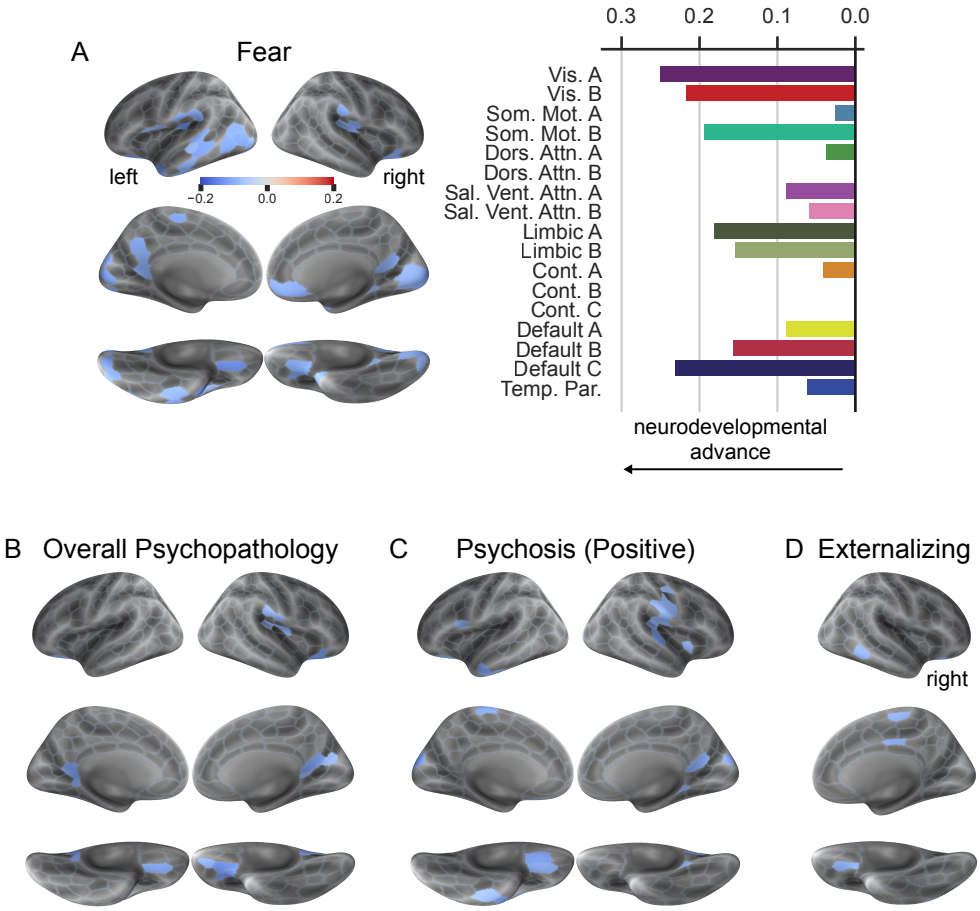

Figure 4. **The relationship between dimensions of psychopathology and deviations from normative neurodevelopment for *cortical thickness* varies over brain systems. A-D**, Significant ρ correlations between the dimension of psychopathology and deviations from the normative model. Negative correlations are interpreted as greater scores on the psychopathology dimension are associated with greater neurodevelopmental advance. Owing to limited effects, the proportion of significant signed effects within each of 17 Yeo brain systems are shown for Fear only. No effects were found in the left hemisphere for Externalizing. *Note*: Only regions where standardized mean squared error was < 1 are presented.

Group effects yield non-specific patterns of deviations from normative neurodevelopment

Having demonstrated that dimensions of psychopathology track variation in regionally specific neurodevelopmental abnormalities, we next examined the extent to which overall psychopathology accounted for overlap between group-level differences observed for traditional case-control analyses in depression and ADHD groups. Figure 5A shows the distribution of Cohen's D values for ADHD and depression for cortical volume with and without controlling for overall psychopathology. For both groups, controlling for overall psychopathology resulted in a significant shift in the Cohen's *D* distribution towards zero (ADHD, $t = 40.92$, $p <$

0.001; depression, $t = 40.97$, $p < 0.001$). Figure 5B shows the relationship between regional Cohen's *D* values in each group without controlling for overall psychopathology ($r = 0.40$, $p < 0.001$), while Figure 5C shows the relationship between regional Cohen's *D* when the effect of overall psychopathology was controlled for ($r = 0.18$, $p < 0.001$). Notably, controlling for overall psychopathology reduced the correlation between depression and ADHD to $r = 0.18$; a delta of 0.22. We repeated this analysis using each of the other psychopathology dimensions and found that this finding was specific to overall psychopathology; when controlling for other dimensions, the next largest reduction in spatial correlation was 0.04 for psychosis-positive ($r = 0.36$, $p < 0.001$).

Figures 5D-F show the same analysis described above for cortical thickness. While Cohen's *D* values were in general smaller for thickness compared to volume, controlling for overall psychopathology still resulted in a significant shift towards zero (Figure 5D; ADHD, $t = 9.17$, $p < 0.001$; depression, $t = 9.04$, $p < 0.001$). Furthermore, the correlation between Cohen's *D* values across groups reduced when controlling for overall psychopathology (Figure 5E, 5F). Together, these results suggest that spatial correspondence between group-level deviations was explained to a large extent by overall psychopathology for both thickness and volume. However, a significant correlation between depression and ADHD remained for both brain thickness and volume after controlling for overall psychopathology, demonstrating persistent overlap between these clinically dissimilar groups.

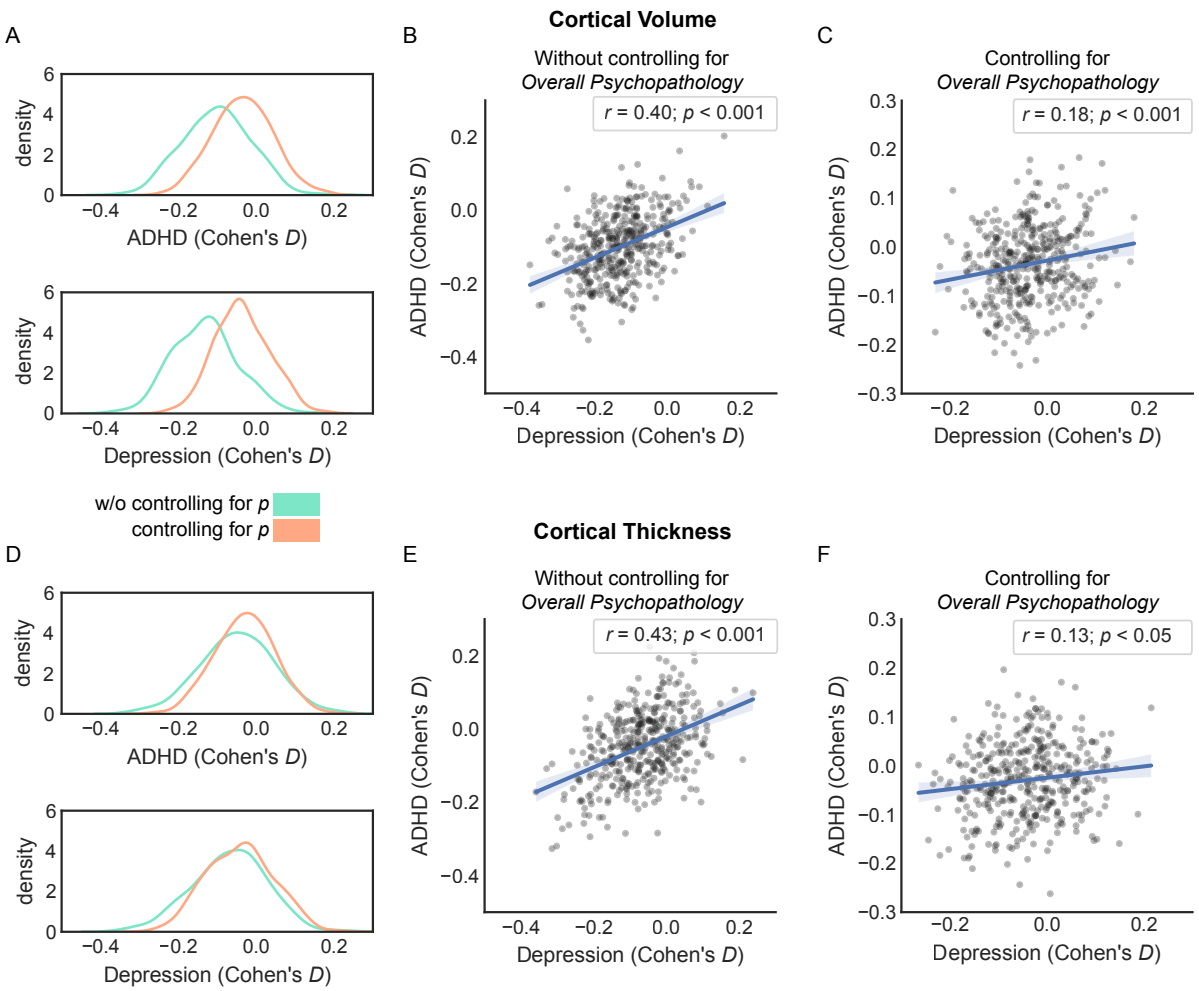

Figure 5. **Group level deviations from normative neurodevelopment in depression and ADHD groups show correlated whole-brain effects confounded by overall psychopathology.** Case-control comparisons were conducted examining group differences in deviations between individuals with depression and individuals with ADHD with healthy individuals from the *train* subset. **A-C**, Results for cortical volume. **D-F**, Results for cortical thickness. **A,D,** Regional Cohen's D values from the ADHD group (top) and depression group (bottom) with and without controlling for overall psychopathology. For both volume and thickness and both groups, controlling for overall psychopathology resulted in a significant shift in Cohen's D values towards zero. **B.E**, Regional Cohen's D values from the depression group correlate to regional Cohen's D values from the ADHD group. **C,F**, Correlations between depression and ADHD groups decrease when controlling for overall psychopathology.

DISCUSSION

Mental disorders are increasingly viewed as disorders of neurodevelopment (3–5,49). However, heterogeneity in both neurodevelopmental trajectories and symptom profiles have confounded case-control designs and made it difficult to precisely identify which neurodevelopmental abnormalities explain specific forms of psychopathology. Here, we showed that distinct dimensions of psychopathology that cut across diagnostic boundaries (25) track deviations from normative neurodevelopment in a large sample of youth. Higher scores on distinct psychopathology dimensions corresponded to spatially varied patterns of regional abnormalities in neurodevelopment. As expected, overall psychopathology correlated with neurodevelopmentally advanced gray matter volume reductions in vmPFC/mOFC, inferior temporal, daCC, and insula cortices, all regions previously implicated in case-control literature across a broad spectrum of disorders (39,40). Additionally, case-control comparisons between two clinically dissimilar groups (depression and ADHD) and our normative sample showed spatially correlated group differences in deviations from neurodevelopment that diminished when controlling for overall psychopathology, suggesting that overall psychopathology confounded case-control comparisons. Overall, our results demonstrate that *p-factor* models of psychopathology, which decouple specific dimensions psychopathology from overall psychopathology, provide novel insights into the pathophysiology of psychiatric conditions.

Previous studies have revealed non-uniform gray matter reductions concentrated in vmPFC/mOFC (Default A in our study), inferior temporal (Default C), daCC (Default & Salience/Ventral Attention) and insula cortices across major depressive, bipolar, schizophrenia, and anxiety disorders (39,40). Here, we found that each of these regions were implicated by overall psychopathology. Further, while the daCC was implicated by overall psychopathology, effects in this region were largely absent for the psychosis and anxious-misery dimensions. This finding suggests that the effects reported in the literature for the daCC may reflect the general neural correlates of mental disorder rather than a disorder-specific signature (39). Additionally, the patterns of neurodevelopmental abnormalities observed for

the psychosis dimensions were distinct from those observed for anxious-misery. While neurodevelopmentally-advanced volume reductions in the lateral OFC and inferior temporal cortex were present in the psychosis dimensions, particularly for psychosis-positive, these effects were not present for anxious-misery, which instead showed scattered neurodevelopmentally-delayed volume reductions. This pattern of results suggests that, when considering the psychosis and anxious-misery dimensions, only the psychosis dimensions were associated with advanced volume reductions in the OFC and inferior temporal cortex beyond the effects observed for overall psychopathology. Thus, abnormalities in these regions reported for depression (40) may reflect the neural correlates of overall psychopathology. Together, these results illustrate the capacity for *p-factor* models to isolate candidate biomarkers that are potentially disorder specific from those that are disorder general.

A striking consistency in our results was that the visual systems were broadly implicated for the overall psychopathology, psychosis-positive, psychosis-negative, and fear dimensions. This observation is consistent with recent functional connectivity work (50,51). Elliot *et al.* (50) showed that overall psychopathology correlated with dysconnectivity between the visual systems and the frontoparietal and default mode systems, and Kebets *et al.* (51) showed that overall psychopathology correlated with dysconnectivity within and between somatomotor and visual systems. Although there are several clear differences between the studies of Elliot *et al.* and Kebets *et al.* and the current study, including neuroimaging modality, clinical assessments, statistical methodology, and sample age, the results converge on the idea that disruptions to lower-order brain systems are common across mental disorders. Given that our sample, and the sample used by Elliot *et al.,* were both younger than that used by Kebets *et al.*, our results may represent an early phase of disease progression that, together with later dysfunction in the somatomotor system, are common across most disorders. Datasets covering the lifespan will be critical to test this hypothesis directly. Notably, our results suggest that lower-order systems, while important, may be less likely than higher-order systems to yield discriminatory utility for mental health.

We observed an inconsistency between our results and that of recent structural work by Romer *et al.* (24). While we found widespread significant correlations between overall psychopathology and cortical volume and relatively few effects for cortical thickness, Romer *et al.* found overall psychopathology yielded widespread correlations with cortical thickness and relatively few for volume (and surface area). This discrepancy may be due to differences in data processing. Here, we derived estimates of cortical thickness using ANTs, while Romer *at al.* used FreeSurfer (FS) via the Human Connectome Project (HCP) minimal preprocessing pipeline. Regional correlations between ANTs-derived and FS-derived cortical thickness estimates are, on average, only moderately correlated (r = ~0.45) (52), demonstrating that there is a lot of unique variance between software packages. Critically, ANTs has been shown to perform better for out-of-sample age and gender prediction when compared to FS (53), suggesting ANTs-derived metrics may be more relevant for analyzing individual differences. An additional difference between our study and that of Romer *et al.* is age of sample; Romer *et al.* studied midlife adults while the current study examined developing youths. Thus, discrepant results may instead suggest that inter-individual differences in different structural properties of the cortex are relevant to psychopathology at different points throughout the lifespan.

Apart from overall psychopathology, we found that cortical volume yielded more significant correlations compared to cortical thickness for each of our other psychopathology dimensions as well. For example, while both of the psychosis dimensions were associated with widespread neurodevelopmentally advanced volume reductions across the cortex, the same was not true for cortical thickness, which showed only scattered effects for the psychosis-positive dimension. This pattern of findings is consistent with previous case-control work demonstrating cortical volume abnormalities in the absence of corresponding cortical thickness changes in schizophrenia (54). Our results suggest that building accurate predictive models of psychopathology throughout development will require multiple assays of brain structure.

Limitations

A limitation of this study is the use of cross-sectional data to model neurodevelopment. It is well documented that individual variability in neurodevelopment occurs at both the inter- and intra-individual level (2), and characterizing the factors that explain the latter will be critical for predicting the emergence of psychopathology over time. Thus, future work should test whether the brain regions identified using our approach explain variance in psychopathology dimensions at follow-up timepoints. Another limitation is the focus on T1-weighted cortical brain features. The underlying white matter pathways change throughout development in parallel with the cortex, giving rise to segregated processing modules that increase the functional efficiency of the brain (55–57). Here, we focused on T1-weighted metrics owing to their robust relationship with age, which makes them well suited for normative models. Lastly, we focused on properties of gray matter derived from voxel data and as such did not examine cortical surface area, a property dependent on vertex data. Given the observed differences between thickness and volume in our results, and discordance with recent literature (24), further examination of, and direct comparison between, voxel and vertex estimates of cortical gray matter will be crucial for building a complete picture of the structural abnormalities associated with psychopathology.

Conclusions

Our results represent an important step toward understanding the link between neurodevelopment and psychopathology. We explicitly modeled normative variance in neurodevelopment, allowing us to estimate continuous single-subject neurodevelopmental abnormalities. Combining this approach with a dimensional model of psychopathology allowed us to uncover spatially varied patterns of neurodevelopmental abnormalities associated with distinct psychopathology dimensions. Critically, our work underscores the importance of decoupling specific forms of psychopathology from overall psychopathology and that not doing so may confound case-control designs, rendering them less likely to yield clinically useful biomarkers in psychiatry. Our work contributes to a growing body of literature demonstrating that, in order to discover neurodevelopmental biomarkers for mental

health, psychiatric research could benefit from supplementing examination of the statistical ‘average patient’ with dimensional approaches to psychopathology and brain pathophysiology (14,15,27). Such a neurobiologically-grounded framework may provide a step towards personalized medicine in psychiatry, and ultimately allow for improved outcome for patients.

CITATION DIVERSITY STATEMENT

Recent work in neuroscience and other fields has identified a bias in citation practices such that papers from women and other minorities are under-cited relative to the number of such papers in the field (58–61). We sought to proactively consider choosing references that reflect the diversity of the field in thought, form of contribution, gender, and other factors. We obtained predicted gender of the first and last author of each reference by using databases that store the probability of a name being carried by a woman (58,62). By this measure (and excluding self-citations to the first and last authors of our current paper), our references contain 9.3% woman(first)/woman(last), 14% man/woman, 23.3% woman/man, 46.5% man/man, and 6.98% unknown categorization. This method is limited in that a) names, pronouns, and social media profiles used to construct the databases may not, in every case, be indicative of gender identity and b) it cannot account for intersex, non-binary, or transgender people. We look forward to future work that could help us to better understand how to support equitable practices in science.

ACKNOWLEDGMENTS

This study was supported by grants from the National Institute of Mental Health: R21MH106799 (D.S.B. & T.D.S.), R01MH113550 (T.D.S. & D.S.B.), and RF1MH116920 (T.D.S. & D.S.B.). Additional support was provided by R01MH120482 (T.D.S.), R01MH107703 (T.D.S.), the John D. and Catherine T. MacArthur Foundation (D.S.B.), the Army Research Office contracts W911NF-14-1-0679 and W911NF-16-1-0474 (D.S.B.), the Army Research Laboratory contract W911NF-10-2-0022 (D.S.B.), R01MH107235 (R.C.G.), K01MH102609 (D.R.R.), R01MH113565 (D.H.W.) and the Penn-CHOP Lifespan Brain Institute. The PNC was supported by RC2MH089983 and RC2MH089924. The authors acknowledge Dr. Graham Baum for data processing as well as Dr. Urs Braun for valuable discussions during the writing of the manuscript.

CONFLICT OF INTEREST

The authors declare no conflict of interest.

REFERENCES:

1. Blakemore S-J, Choudhury S (2006): Development of the adolescent brain: implications for executive function and social cognition. *J Child Psychol & Psychiat* 47: 296–312.
2. Foulkes L, Blakemore S-J (2018): Studying individual differences in human adolescent brain development. *Nat Neurosci* 21: 315–323.
3. Paus T, Keshavan M, Giedd JN (2008): Why do many psychiatric disorders emerge during adolescence? *Nat Rev Neurosci* 9: 947–957.
4. Bassett DS, Xia CH, Satterthwaite TD (2018): Understanding the Emergence of Neuropsychiatric Disorders With Network Neuroscience. *Biological Psychiatry: Cognitive Neuroscience and Neuroimaging* 3: 742–753.
5. Ball G, Beare R, Seal ML (2017): Network component analysis reveals developmental trajectories of structural connectivity and specific alterations in autism spectrum disorder: Network Component Analysis with NMF. *Human Brain Mapping* 38: 4169–4184.
6. Fried EI (2015): Depression is not a consistent syndrome_ An investigation of unique symptom patterns in the STAR*D study. *Journal of Affective Disorders* 7.
7. Jacobi F, Wittchen H-U, Hölting C, Höfler M, Pfister H, Müller N, Lieb R (2004): Prevalence, co-morbidity and correlates of mental disorders in the general population: results from the German Health Interview and Examination Survey (GHS). *Psychol Med* 34: 597–611.
8. Hasin D, Kilcoyne B (2012): Comorbidity of psychiatric and substance use disorders in the United States: current issues and findings from the NESARC. *Current Opinion in Psychiatry* 25: 165–171.
9. Kessler RC, Berglund P, Demler O, Jin R, Merikangas KR, Walters EE (2005): Lifetime Prevalence and Age-of-Onset Distributions of DSM-IV Disorders in the National Comorbidity Survey Replication. *Arch Gen Psychiatry* 62: 593.
10. Lahey BB, Applegate B, Hakes JK, Zald DH, Hariri AR, Rathouz PJ (2012): Is there a general factor of prevalent psychopathology during adulthood? *Journal of Abnormal Psychology* 121: 971–977.

11. Insel T, Cuthbert B, Garvey M, Heinssen R, Pine DS, Quinn K, *et al.* (2010): Research Domain Criteria (RDoC): Toward a New Classification Framework for Research on Mental Disorders. *AJP* 167: 748–751.
12. Casey BJ, Craddock N, Cuthbert BN, Hyman SE, Lee FS, Ressler KJ (2013): DSM-5 and RDoC: progress in psychiatry research? *Nat Rev Neurosci* 14: 810–814.
13. Cuthbert BN, Insel TR (2013): Toward the future of psychiatric diagnosis: the seven pillars of RDoC. *BMC Med* 11: 126.
14. Marquand AF, Wolfers T, Dinga R (2019): Phenomapping: Methods and Measures for Deconstructing Diagnosis in Psychiatry. In: Passos IC, Mwangi B, Kapczinski F, editors. *Personalized Psychiatry*. Cham: Springer International Publishing, pp 119–134.
15. Marquand AF, Kia SM, Zabihi M, Wolfers T, Buitelaar JK, Beckmann CF (2019): Conceptualizing mental disorders as deviations from normative functioning. *Mol Psychiatry*. https://doi.org/10.1038/s41380-019-0441-1
16. Parkes L, Tiego J, Aquino K, Braganza L, Chamberlain SR, Fontenelle LF, *et al.* (2019): Transdiagnostic variations in impulsivity and compulsivity in obsessive-compulsive disorder and gambling disorder correlate with effective connectivity in cortical-striatal-thalamic-cortical circuits. *NeuroImage* 202: 116070.
17. Moore TM, Calkins ME, Satterthwaite TD, Roalf DR, Rosen AFG, Gur RC, Gur RE (2019): Development of a computerized adaptive screening tool for overall psychopathology ("p"). *Journal of Psychiatric Research* 116: 26–33.
18. Caspi A, Houts RM, Belsky DW, Goldman-Mellor SJ, Harrington H, Israel S, *et al.* (2014): The p Factor: One General Psychopathology Factor in the Structure of Psychiatric Disorders? *Clinical Psychological Science* 2: 119–137.
19. Caspi A, Moffitt TE (2018): All for One and One for All: Mental Disorders in One Dimension. *AJP* 175: 831–844.
20. Reise SP, Moore TM, Haviland MG (2010): Bifactor Models and Rotations: Exploring the Extent to Which Multidimensional Data Yield Univocal Scale Scores. *Journal of Personality Assessment* 92: 544–559.

21. Kaczkurkin AN, Park SS, Sotiras A, Moore TM, Calkins ME, Cieslak M, *et al.* (2019): Evidence for Dissociable Linkage of Dimensions of Psychopathology to Brain Structure in Youths. *AJP* appi.ajp.2019.1.
22. Romer AL, Knodt AR, Houts R, Brigidi BD, Moffitt TE, Caspi A, Hariri AR (2018): Structural alterations within cerebellar circuitry are associated with general liability for common mental disorders. *Mol Psychiatry* 23: 1084–1090.
23. Romer AL, Knodt AR, Sison ML, Ireland D, Houts R, Ramrakha S, *et al.* (2019): Replicability of structural brain alterations associated with general psychopathology: evidence from a population-representative birth cohort. *Mol Psychiatry*. https://doi.org/10.1038/s41380-019-0621-z
24. Romer AL, Elliott ML, Knodt AR, Sison ML, Ireland D, Houts R, *et al.* (2020): Pervasively Thinner Neocortex as a Transdiagnostic Feature of General Psychopathology. *AJP* appi.ajp.2020.1.
25. Calkins ME, Merikangas KR, Moore TM, Burstein M, Behr MA, Satterthwaite TD, *et al.* (2015): The Philadelphia Neurodevelopmental Cohort: constructing a deep phenotyping collaborative. *J Child Psychol Psychiatr* 56: 1356–1369.
26. Shanmugan S, Wolf DH, Calkins ME, Moore TM, Ruparel K, Hopson RD, *et al.* (2016): Common and Dissociable Mechanisms of Executive System Dysfunction Across Psychiatric Disorders in Youth. *American Journal of Psychiatry* 173: 517–526.
27. Marquand AF, Rezek I, Buitelaar J, Beckmann CF (2016): Understanding Heterogeneity in Clinical Cohorts Using Normative Models: Beyond Case-Control Studies. *Biological Psychiatry* 80: 552–561.
28. Wolfers T, Doan NT, Kaufmann T, Alnæs D, Moberget T, Agartz I, *et al.* (2018): Mapping the Heterogeneous Phenotype of Schizophrenia and Bipolar Disorder Using Normative Models. *JAMA Psychiatry* 75: 1146.
29. Wolfers T, Beckmann CF, Hoogman M, Buitelaar JK, Franke B, Marquand AF (2019): Individual differences v. the average patient: mapping the heterogeneity in ADHD using normative models. *Psychological Medicine* 1–10.
30. Zabihi M, Oldehinkel M, Wolfers T, Frouin V, Goyard D, Loth E, *et al.* (2018): Dissecting the Heterogeneous Cortical Anatomy of Autism Spectrum

Disorder Using Normative Models. *Biological Psychiatry: Cognitive Neuroscience and Neuroimaging*. https://doi.org/10.1016/j.bpsc.2018.11.013

31. Mills KL, Goddings A-L, Herting MM, Meuwese R, Blakemore S-J, Crone EA, *et al.* (2016): Structural brain development between childhood and adulthood: Convergence across four longitudinal samples. *NeuroImage* 141: 273–281.
32. Alexander-Bloch A, Raznahan A, Bullmore E, Giedd J (2013): The Convergence of Maturational Change and Structural Covariance in Human Cortical Networks. *Journal of Neuroscience* 33: 2889–2899.
33. Wierenga LM, Langen M, Oranje B, Durston S (2014): Unique developmental trajectories of cortical thickness and surface area. *NeuroImage* 87: 120–126.
34. Tamnes CK, Herting MM, Goddings A-L, Meuwese R, Blakemore S-J, Dahl RE, *et al.* (2017): Development of the Cerebral Cortex across Adolescence: A Multisample Study of Inter-Related Longitudinal Changes in Cortical Volume, Surface Area, and Thickness. *J Neurosci* 37: 3402–3412.
35. Han LK, Dinga R, Hahn T, Ching C, Eyler L, Aftanas L, *et al.* (2019): *Brain Aging in Major Depressive Disorder: Results from the ENIGMA Major Depressive Disorder Working Group*. Neuroscience. https://doi.org/10.1101/560623
36. for the ENIGMA-Major Depressive Disorder Working Group, Schmaal L, Hibar DP, Sämann PG, Hall GB, Baune BT, *et al.* (2017): Cortical abnormalities in adults and adolescents with major depression based on brain scans from 20 cohorts worldwide in the ENIGMA Major Depressive Disorder Working Group. *Mol Psychiatry* 22: 900–909.
37. van Erp TGM, Walton E, Hibar DP, Schmaal L, Jiang W, Glahn DC, *et al.* (2018): Cortical Brain Abnormalities in 4474 Individuals With Schizophrenia and 5098 Control Subjects via the Enhancing Neuro Imaging Genetics Through Meta Analysis (ENIGMA) Consortium. *Biological Psychiatry* 84: 644–654.
38. for the ENIGMA Bipolar Disorder Working Group, Hibar DP, Westlye LT, Doan NT, Jahanshad N, Cheung JW, *et al.* (2018): Cortical abnormalities in bipolar disorder: an MRI analysis of 6503 individuals from the ENIGMA Bipolar Disorder Working Group. *Mol Psychiatry* 23: 932–942.

39. Goodkind M, Eickhoff SB, Oathes DJ, Jiang Y, Chang A, Jones-Hagata LB, *et al.* (2015): Identification of a Common Neurobiological Substrate for Mental Illness. *JAMA Psychiatry* 72: 305.
40. Schmaal L, Pozzi E, C. Ho T, van Velzen LS, Veer IM, Opel N, *et al.* (2020): ENIGMA MDD: seven years of global neuroimaging studies of major depression through worldwide data sharing. *Transl Psychiatry* 10: 172.
41. Satterthwaite TD, Elliott MA, Ruparel K, Loughead J, Prabhakaran K, Calkins ME, *et al.* (2014): Neuroimaging of the Philadelphia Neurodevelopmental Cohort. *NeuroImage* 86: 544–553.
42. Calkins ME, Moore TM, Merikangas KR, Burstein M, Satterthwaite TD, Bilker WB, *et al.* (2014): The psychosis spectrum in a young U.S. community sample: findings from the Philadelphia Neurodevelopmental Cohort. - 13: 296–305.
43. Kaczkurkin AN, Moore TM, Calkins ME, Ciric R, Detre JA, Elliott MA, *et al.* (2018): Common and dissociable regional cerebral blood flow differences associate with dimensions of psychopathology across categorical diagnoses. *Molecular Psychiatry* 23: 1981–1989.
44. Sabaroedin K, Tiego J, Parkes L, Sforazzini F, Finlay A, Johnson B, *et al.* (2019): Functional Connectivity of Corticostriatal Circuitry and Psychosis-like Experiences in the General Community. *Biological Psychiatry* 86: 16–24.
45. Schaefer A, Kong R, Gordon EM, Laumann TO, Zuo X-N, Holmes AJ, *et al.* (2018): Local-Global Parcellation of the Human Cerebral Cortex from Intrinsic Functional Connectivity MRI. *Cerebral Cortex* 28: 3095–3114.
46. Franke K, Gaser C (2019): Ten Years of BrainAGE as a Neuroimaging Biomarker of Brain Aging: What Insights Have We Gained? *Front Neurol* 10: 789.
47. Benjamini Y, Hochberg Y (1995): Controlling the False Discovery Rate: A Practical and Powerful Approach to Multiple Testing. *Journal of the Royal Statistical Society: Series B (Methodological)* 57: 289–300.
48. Thomas Yeo BT, Krienen FM, Sepulcre J, Sabuncu MR, Lashkari D, Hollinshead M, *et al.* (2011): The organization of the human cerebral cortex estimated by intrinsic functional connectivity. *Journal of Neurophysiology* 106: 1125–1165.

49. Kaufmann T, Alnæs D, Doan NT, Brandt CL, Andreassen OA, Westlye LT (2017): Delayed stabilization and individualization in connectome development are related to psychiatric disorders. *Nature Neuroscience* 20: 513–515.
50. Elliott ML, Romer A, Knodt AR, Hariri AR (2018): A Connectome-wide Functional Signature of Transdiagnostic Risk for Mental Illness. *Biological Psychiatry* 84: 452–459.
51. Kebets V, Holmes AJ, Orban C, Tang S, Li J, Sun N, *et al.* (2019): Somatosensory-Motor Dysconnectivity Spans Multiple Transdiagnostic Dimensions of Psychopathology. *Biological Psychiatry* 86: 779–791.
52. Bhagwat N, Barry A, Dickie EW, Brown ST, Devenyi GA, Hatano K, *et al.* (2020): *Understanding the Impact of Preprocessing Pipelines on Neuroimaging Cortical Surface Analyses*. Bioinformatics. https://doi.org/10.1101/2020.05.22.100180
53. Tustison NJ, Cook PA, Klein A, Song G, Das SR, Duda JT, *et al.* (2014): Large-scale evaluation of ANTs and FreeSurfer cortical thickness measurements. *NeuroImage* 99: 166–179.
54. Kong L, Herold CJ, Zöllner F, Salat DH, Lässer MM, Schmid LA, *et al.* (2015): Comparison of grey matter volume and thickness for analysing cortical changes in chronic schizophrenia: A matter of surface area, grey/white matter intensity contrast, and curvature. *Psychiatry Research: Neuroimaging* 231: 176–183.
55. Baker STE, Lubman DI, Yucel M, Allen NB, Whittle S, Fulcher BD, *et al.* (2015): Developmental Changes in Brain Network Hub Connectivity in Late Adolescence. *Journal of Neuroscience* 35: 9078–9087.
56. Baum GL, Ciric R, Roalf DR, Betzel RF, Moore TM, Shinohara RT, *et al.* (2017): Modular Segregation of Structural Brain Networks Supports the Development of Executive Function in Youth. *Current Biology* 27: 1561-1572.e8.
57. Tang E, Giusti C, Baum GL, Gu S, Pollock E, Kahn AE, *et al.* (2017): Developmental increases in white matter network controllability support a growing diversity of brain dynamics. *Nature Communications* 8. https://doi.org/10.1038/s41467-017-01254-4

58. Dworkin JD, Linn KA, Teich EG, Zurn P, Shinohara RT, Bassett DS (2020): *The Extent and Drivers of Gender Imbalance in Neuroscience Reference Lists*. Scientific Communication and Education. https://doi.org/10.1101/2020.01.03.894378
59. Maliniak D, Powers R, Walter BF (2013): The Gender Citation Gap in International Relations. *Int Org* 67: 889–922.
60. Caplar N, Tacchella S, Birrer S (2017): Quantitative evaluation of gender bias in astronomical publications from citation counts. *Nat Astron* 1: 0141.
61. Dion ML, Sumner JL, Mitchell SM (2018): Gendered Citation Patterns across Political Science and Social Science Methodology Fields. *Polit Anal* 26: 312–327.
62. Zhou D, Cornblath EJ, Stiso J, Teich EG, Dworkin JD, Blevins AS, Bassett DS (2020): Gender Diversity Statement and Code Notebook v1.0. Zenodo. Retrieved from https://doi.org/10.5281/zenodo.3672110

Supplementary Materials: Transdiagnostic dimensions of psychopathology explain individuals' unique deviations from normative neurodevelopment in brain structure

Linden Parkes PhD, Tyler M. Moore PhD, Monica E. Calkins PhD, Philip A. Cook PhD, Matthew Cieslak PhD, David R. Roalf PhD, Daniel H. Wolf MD PhD, Ruben C. Gur PhD, Raquel E. Gur MD PhD, Theodore D. Satterthwaite MD, Danielle S. Bassett PhD

SUPPLEMENTARY METHODS

SUPPLEMENTARY RESULTS

Figure S1. **Regions without reliable effects of age and sex.**

Table S1. Brain regions with significant correlations between psychopathology dimensions and deviations from normative neurodevelopment of cortical volume (*normative*) yield larger effect sizes when compared to direct correlations between dimensions and cortical volume (*conventional*).

Figure S2. **The relationship between dimensions of psychopathology and deviations from normative neurodevelopment for *cortical volume* in the *Schaefer200* parcellation.**

Figure S3. **The relationship between dimensions of psychopathology and deviations from normative neurodevelopment for *cortical thickness* in the *Schaefer200* parcellation.**

Figure S4. **The relationship between dimensions of psychopathology and deviations from normative neurodevelopment for *cortical volume* in the *Lausanne234* parcellation.**

Figure S5. **The relationship between dimensions of psychopathology and deviations from normative neurodevelopment for *cortical thickness* in the *Lausanne234* parcellation.**

Table S2. Factor loadings from bifactor model of psychopathology dimensions

SUPPLEMENTARY METHODS

Participants

From the original 1,601 participants from the Philadelphia Neurodevelopmental Cohort (PNC) (1), 156 were excluded due to the presence of gross radiological abnormalities distorting brain anatomy or due to medical history that might impact brain function; those with a history of psychiatric illness were retained. An additional 51 individuals were excluded because they did not pass rigorous manual and automated quality assurance; one individual was excluded due to corrupted data. This process left a final sample of 1,393 participants. Note that this is a larger sample than studies of normative brain development that have used the PNC; unlike previous reports, we did not exclude based on history of psychiatric illness. Indeed, previous work has illustrated that this broader coverage of the PNC yields prevalence rates of mental disorders consistent with population norms (2). The institutional review boards of both the University of Pennsylvania and the Children's Hospital of Philadelphia approved all study procedures.

Psychopathology phenotypes

In this study, we extended a *p-factor* model that was previously developed based on the GOASSESS interview (3,4) and that has previously been used to study the brain (5–7). Briefly, the GOASSESS is an abbreviated and modified structured interview derived from the NIMH Genetic Epidemiology Research Branch Kiddie-SADS (8) that covers a wide variety of psychiatric symptomatology such as the occurrence of mood (major depressive episode, mania), anxiety (agoraphobia, generalized anxiety, panic, specific phobia, social phobia, separation anxiety, obsessive compulsive disorder), externalizing behavior (oppositional defiant, attention deficit/hyperactivity, conduct disorder), eating disorder (anorexia, bulimia), and suicidal thoughts and behaviors. GOASSESS was administered by trained and certified assessors. The original model used a combination of exploratory and confirmatory factor analysis to distill the 112 item-level symptoms from the GOASSESS into five orthogonal dimensions of psychopathology. The original model included a factor common to all psychiatric disorders, referred to as overall psychopathology, as well as four specific factors: anxious-misery, psychosis, externalizing behaviors, and fear.

Here, owing to emergent evidence that the positive and negative aspects of the psychosis spectrum elicit unique effects on the brain (9), we extended the above *p-factor* model in two ways. First, we included an additional five assessor-rated polytomous items (scored from 0-6, where 0 is 'absent' and 6 is 'severe and psychotic' or 'extreme' from the Scale of Prodromal Symptoms (SOPS) derived from the Structured Interview for Prodromal Syndromes (SIPS (10)) designed to measure the negative/disorganized symptoms of psychosis. These five items were (i) P5 disorganized communication, (ii) N2 avolition, (iii) N3 expression of emotion, (iv) N4 experience of emotions and self, and (v) N6 occupational functioning. Including this additional set brought the total to 117 items. Second, we split the psychosis factor into two factors, one describing the delusions and hallucinations

associated with the psychosis spectrum, which we call psychosis-positive. The second psychosis factor described disorganized thought, cognitive impairments, and motivational-emotional deficits, which we call psychosis-negative for simplicity. We used confirmatory factor analysis implemented in Mplus (11) to model five specific factors of psychopathology (anxious-misery, psychosis-positive, psychosis-negative, externalizing behaviors, and fear) as well as one common factor (overall psychopathology) (Figure 1A). Note that all phenotypes derived from this model are orthogonal to one another.

Imaging data acquisition

MRI data were acquired on a 3 Tesla Siemens Tim Trio scanner with a 32-channel head coil at the Hospital of the University of Pennsylvania. A 5-min magnetization-prepared, rapid acquisition gradient-echo T1-weighted (MPRAGE) image (TR = 1810ms, TE = 3.51ms, FOV = 180 x 240mm, matrix 256 x 192, voxel resolution of $1mm^3$) was acquired for each participant.

Imaging data quality control

All T1-weighted images underwent rigorous quality control by highly trained image analysts, see (12) for details. Briefly, all images were visually inspected and evaluated for the presence of artifacts. Images with gross artifacts were considered unusable; images with some artifacts were flagged as 'decent'; and images free of artifact were marked as 'superior'. As mentioned above in the section titled *Participants*, 208 individuals were removed due to unusable imaging data. As a result, 1,155 of our 1,393 participants had T1-weighted images identified as 'superior', with the remaining identified as 'usable'.

Whole brain parcellation

We summarized each of the brain features examined in the current study at the region level. Analyses reported in the main text were conducted using 400 regions covering the cortex that were defined using functional neuroimaging data in a previous study (13), hereafter referred as the Schaefer400 parcellation. However, there is a plethora of parcellations available in neuroimaging research that vary in their construction and resolution (i.e., number of regions). In light of this diversity, we sought to confirm that our results were not driven by choice of brain parcellation, and thus we repeated our analyses using both a lower resolution version of the Schaefer parcellation that included only 200 regions covering the cortex (Schaefer200), as well as a separate parcellation wherein boundaries were defined according to neuroanatomy rather than brain function (14), including 234 regions (Lausanne234). For each parcellation brain features were generated for each participant as described in the following sections.

Structural image processing

Structural image processing used tools included in ANTs (15). Structural images were processed in participant's native space using the following procedure: brain extraction, N4 bias field correction (16), Atropos tissue segmentation (17), SyN diffeomorphic registration (18,19), and direct estimation of cortical thickness in volumetric space (20). Large-scale evaluation studies have shown that this highly accurate procedure for estimating cortical thickness is more sensitive to individual differences over the lifespan than comparable techniques (15).

Regional estimates of cortical thickness and volume were extracted from every participant's native space data using the following procedure. First, we created a custom adolescent template and tissue priors using data from 140 PNC participants, balanced for age and sex. A custom template minimizes registration bias and maximizes sensitivity to detect regional effects that can be impacted by registration error. Second, the Schaefer400 and Schaefer200 parcellations were generated in this template space. Third, non-linear registration warps were generated that mapped each participant's structural scan to template space, and the inverse of these warps were applied to the Schaefer parcellations to generate participant-specific parcellations. Participant-specific Lausanne234 parcellations were generated in native space data using code available online: https://github.com/mattcieslak/easy_lausanne. Fourth, each participant's Schaefer parcellation was masked by a cortical gray matter mask from ANTs, also in participant's native space. Finally, regional cortical thickness estimates were extracted using these participant-specific parcellations (Schafer400, Schaefer200, Lausanne234); a count of the number of voxels in each parcel in native space served as an estimate of regional volume. For the Schaefer400 parcellation, these features were assembled into a 1,393 × 800 feature table, $\boldsymbol{F}$, with brain regions along the columns, each represented twice to account for thickness and volume, and participants along the rows.

Permutation test

As mentioned in the main text, for each psychopathology phenotype we generated whole-brain correlation maps that quantified the relationship between a given psychopathology phenotype and deviations from normative neurodevelopment for each measure of cortical thickness and volume. We used a random permutation procedure to assign *p*-values to these correlation maps. Specifically, the psychopathology phenotypes were randomly shuffled and the correlation coefficients ρ were recalculated between the permuted psychopathology phenotypes and the columns of $\boldsymbol{F_z}$. Note, the unpermuted psychopathology phenotypes were already residualized with respect to age and sex. This was repeated 1,000 times to generate an empirical null distribution for every psychopathology phenotype-brain feature pair. *p*-values were calculated as the proportion of absolute ρ values from the empirical null that were greater than or equal to the absolute observed ρ value for a given psychopathology phenotype and brain feature.

When considering the parcellation used in the main text (Schaefer400), the above permutation procedure generated 400 uncorrected *p*-values per psychopathology dimension and brain feature. Considering our derivation of six psychopathology phenotypes, this translated to 2,400 uncorrected *p*-values for each of cortical thickness and cortical volume. Multiple comparisons were corrected for across brain regions and psychopathology dimensions by adjusting the 2,400 *p*-values using the Benjamini and Hochberg False Discovery Rate (FDR, $q = 0.05$) procedure (21). Next, we discarded brain regions where the standardized mean squared error from the normative model was ≥ 1 (Figure S1), ensuring that our correlations of psychopathology dimensions to deviations were not testing for effects where no reliable age effect was present. This multiple comparison correction procedure was applied to cortical volume and thickness separately.

Comparison of effect sizes to traditional analysis of inter-individual differences

Primary analysis in the main text were done by correlating dimensions of psychopathology with deviations from a normative model of neurodevelopment estimated using gaussian process regression. To test the utility of the normative model in our primary analysis, we also conducted a *conventional* analysis of inter-individual differences, wherein each psychopathology dimension was correlated directly with regional brain features rather than deviations from the normative model. In this analysis, age and sex were controlled for in the full sample using ordinary least squares linear regression. As per our primary analysis, significance was assigned using the same permutation test outlined above (see section titled *Permutation test*) and rigorously corrected for multiple comparisons across regions and psychopathology dimensions using FDR.

In order to directly compare to two correlation analyses (normative model and conventional) we performed regional comparisons of the significant ρ values using Steiger's test for dependent correlations (22). Specifically, for each psychopathology dimension, we selected the subset of regions that showed both significant correlations with deviations from the normative model as well as in the conventional analysis (i.e., the intersection). Then, we compared the ρ value pairs within each region to see which analysis yielded the significantly larger effect size. Steiger's test *p*-values were assigned parametrically and corrected for multiple comparisons using FDR.

SUPPLEMENTARY RESULTS

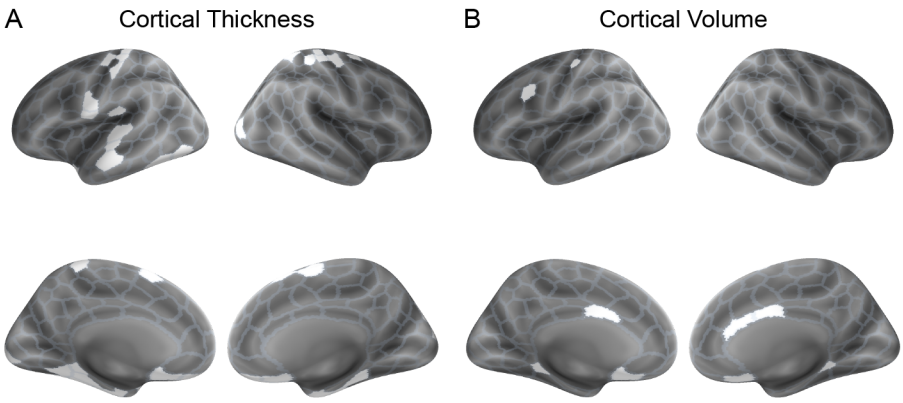

Figure S1. **Regions without reliable effects of age and sex.** Regions with standardized mean squared error of ≥ 1 are shown in white for cortical thickness (**A**) and cortical volume (**B**). These regions were excluded from all analyses reported in this study.

Comparison of effect sizes to traditional analysis of inter-individual differences

To test the extent to which our normative model yielded stronger correlations to psychopathology, we also performed a *conventional* analysis of inter-individual differences by estimating direct correlations between our dimensions of psychopathology and brain features. We examined the subset of regions where significant effects were found in *both* the normative model and the conventional model. The proportion of this subset that had significantly larger effect sizes in one analysis or the other is shown in Table S1. We find that for overall psychopathology, psychosis-positive, and fear, a greater proportion of regions showed significantly greater ρ values, under the Steiger's test, when dimensions were correlated with deviations from the normative model rather than directly with cortical volume. No significant differences in effect sizes were observed for psychosis-negative, anxious-misery, or externalizing.

Table S1. Brain regions with significant correlations between psychopathology dimensions and deviations from normative neurodevelopment of cortical volume (*normative*) yield larger effect sizes when compared to direct correlations between dimensions and cortical volume (*conventional*).

	Ov. Psych.	Psy. (pos.)	Fear
Number of regions in subset (Number of brain regions = 400)	118	53	83
Significantly larger ρ values in the *normative* model (% of subset)	10.17	20.75	13.25
Significantly larger ρ values in the *conventional* analysis (% of subset)	3.39	1.89	0

Note Steiger's test *p*-values were corrected using FDR (q = 0.05).

Sensitivity analyses

Parcellation scheme

In the main text, we reported results for Schaefer400. Here, we report our results according to a Schaefer parcellation with only 200 regions (Cortical Volume, Figure S2; Cortical Thickness, Figure S3) as well as an entirely different parcellation known as the Lausanne atlas with 234 regions (Cortical Volume, Figure S4; Cortical Thickness, Figure S5).

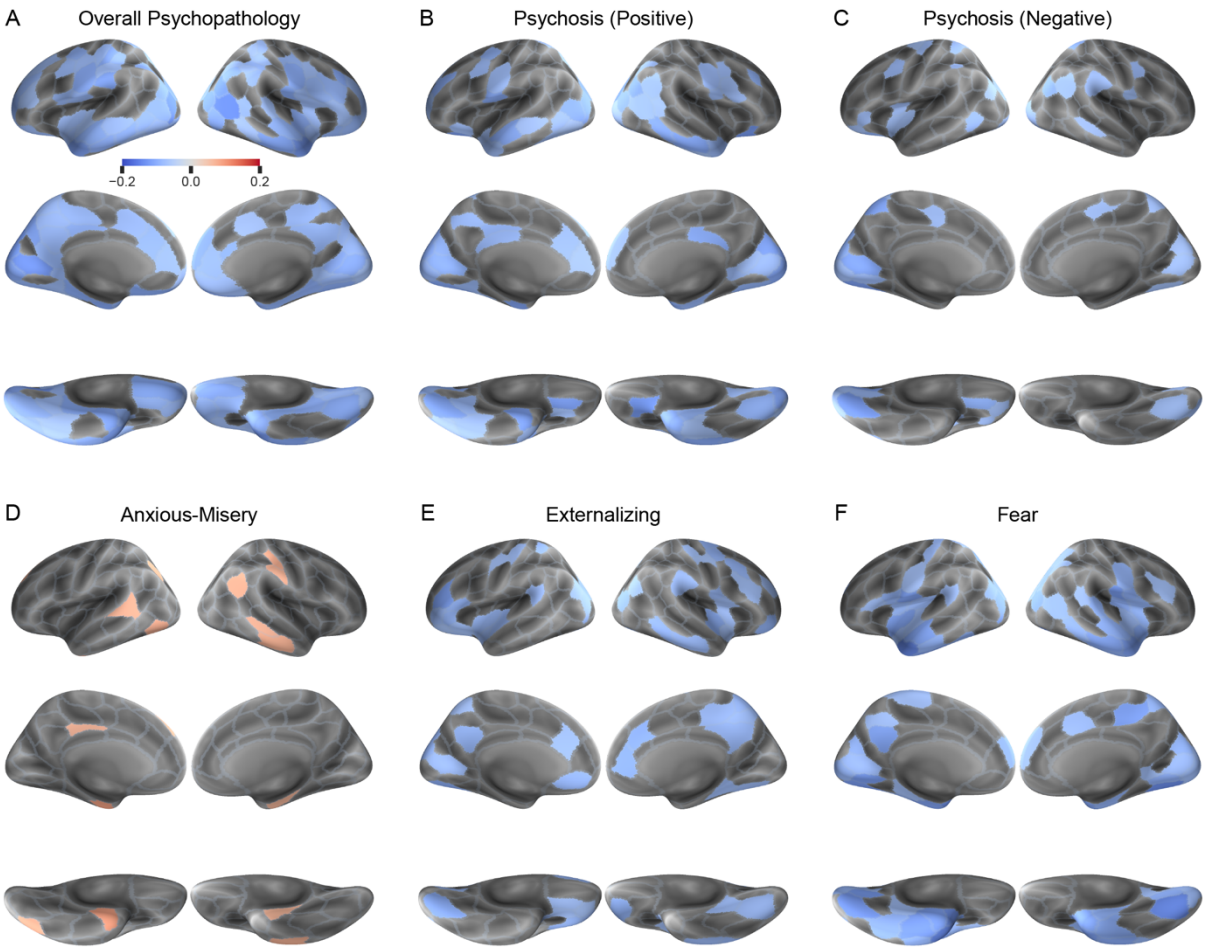

Figure S2. **The relationship between dimensions of psychopathology and deviations from normative neurodevelopment for *cortical volume* in the *Schaefer200* parcellation. A-F**, Significant ρ correlations between the dimension of psychopathology and deviations from the normative model. Psychopathology dimensions not shown had no significant correlations.

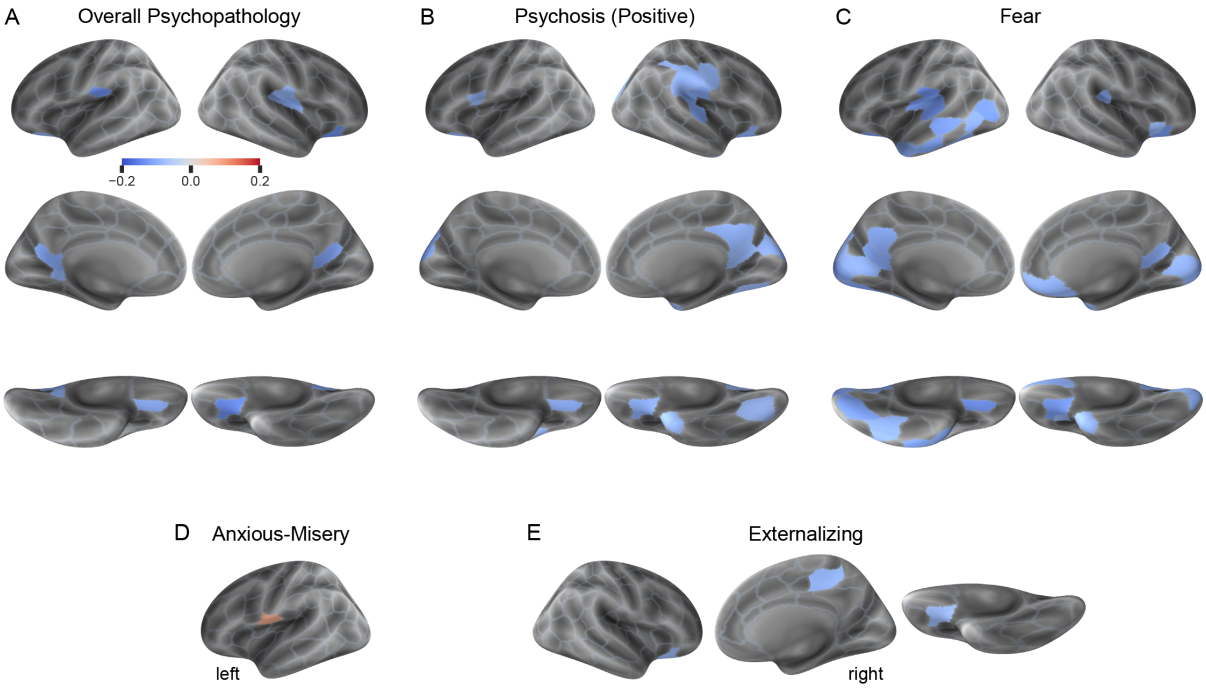

Figure S3. **The relationship between dimensions of psychopathology and deviations from normative neurodevelopment for *cortical thickness* in the *Schaefer200* parcellation. A-C**, Significant ρ correlations between the dimension of psychopathology and deviations from the normative model. Psychopathology dimensions not shown had no significant correlations.

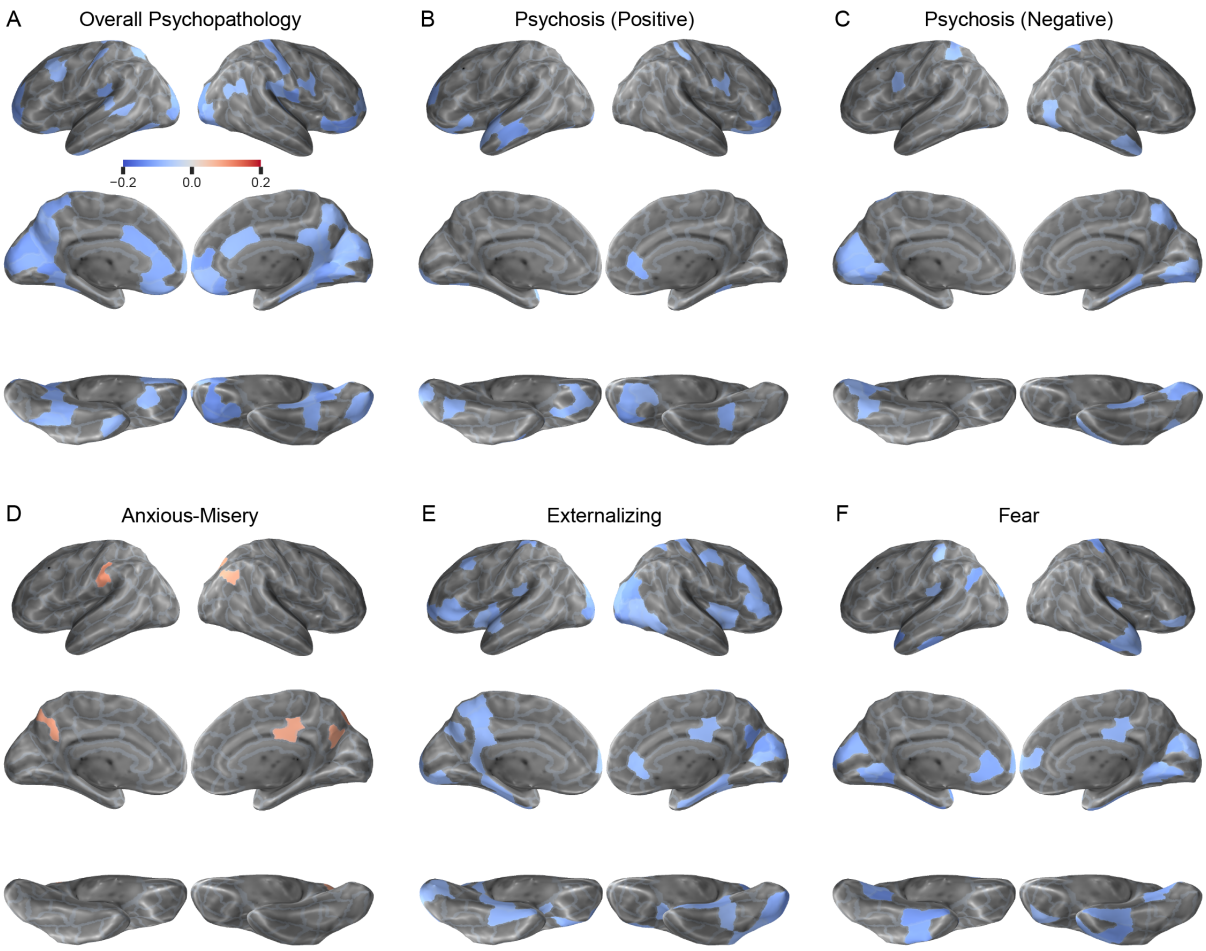

Figure S4. **The relationship between dimensions of psychopathology and deviations from normative neurodevelopment for *cortical volume* in the *Lausanne234* parcellation. A-F**, Significant ρ correlations between the dimension of psychopathology and deviations from the normative model. Psychopathology dimensions not shown had no significant correlations.

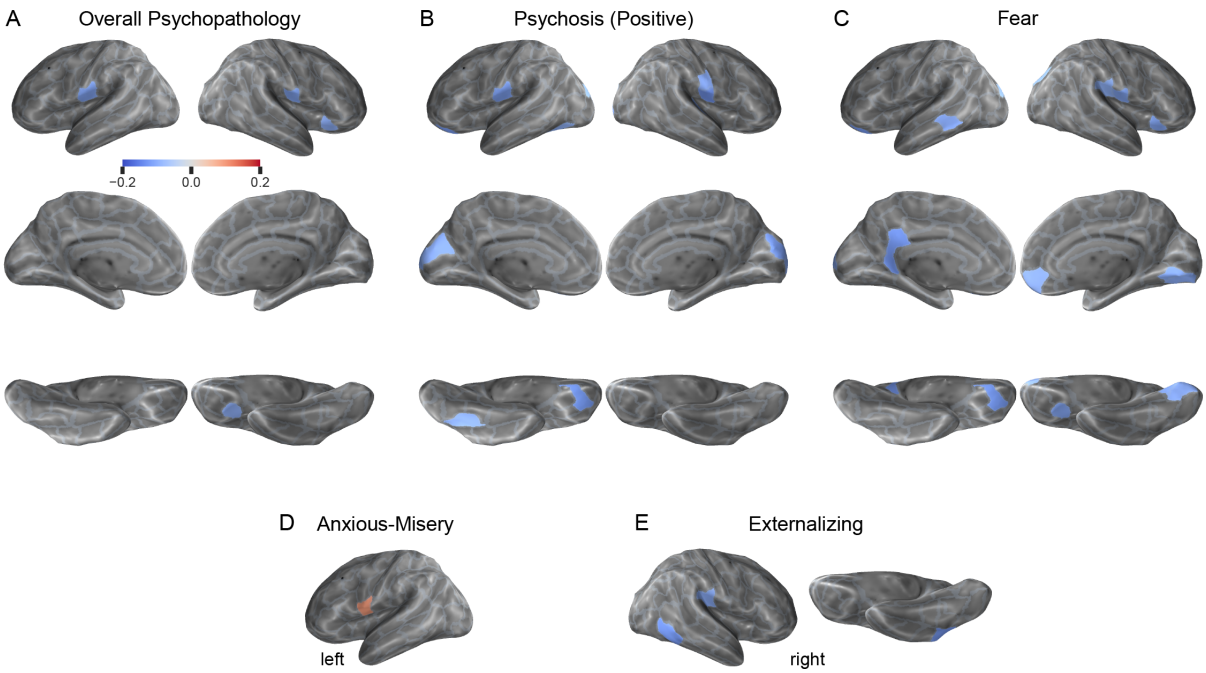

Figure S5. **The relationship between dimensions of psychopathology and deviations from normative neurodevelopment for *cortical thickness* in the *Lausanne234* parcellation. A-E**, Significant ρ correlations between the dimension of psychopathology and deviations from the normative model. Psychopathology dimensions and hemispheres not shown had no significant correlations.

Table S2. Factor loadings from bifactor model of psychopathology dimensions

	Loadings					
Item	General	Psychosis Positive	Psychosis Negative	Anxious-Misery	Externalizing	Fear
psy001	**0.657**	**0.442**	0.000	0.000	0.000	0.000
psy029	**0.606**	**0.411**	0.000	0.000	0.000	0.000
psy050	**0.632**	**0.220**	0.000	0.000	0.000	0.000
psy060	**0.666**	**0.316**	0.000	0.000	0.000	0.000
psy070	**0.637**	**0.285**	0.000	0.000	0.000	0.000
psy071	**0.721**	**0.187**	0.000	0.000	0.000	0.000
sip003	**0.598**	**0.522**	0.000	0.000	0.000	0.000
sip004	**0.422**	**0.616**	0.000	0.000	0.000	0.000
sip005	**0.593**	**0.605**	0.000	0.000	0.000	0.000
sip006	**0.557**	**0.559**	0.000	0.000	0.000	0.000
sip007	**0.584**	**0.608**	0.000	0.000	0.000	0.000
sip008	**0.519**	**0.628**	0.000	0.000	0.000	0.000
sip009	**0.615**	**0.502**	0.000	0.000	0.000	0.000
sip010	**0.437**	**0.666**	0.000	0.000	0.000	0.000
sip011	**0.623**	**0.607**	0.000	0.000	0.000	0.000
sip012	**0.639**	**0.596**	0.000	0.000	0.000	0.000
sip013	**0.605**	**0.593**	0.000	0.000	0.000	0.000
sip014	**0.715**	**0.489**	0.000	0.000	0.000	0.000
sip027	**0.487**	0.000	**0.288**	0.000	0.000	0.000
sip028	**0.517**	0.000	**0.305**	0.000	0.000	0.000
sip032	**0.758**	0.000	**0.188**	0.000	0.000	0.000
sip033	**0.681**	0.000	**0.205**	0.000	0.000	0.000
sip038	**0.396**	0.000	**0.795**	0.000	0.000	0.000
sip039	**0.483**	0.000	**0.631**	0.000	0.000	0.000
SIP030	**0.524**	0.000	**0.383**	0.000	0.000	0.000
SIP035	**0.714**	0.000	**0.302**	0.000	0.000	0.000
SIP037	**0.387**	0.000	**0.395**	0.000	0.000	0.000
SIP041	**0.459**	0.000	**0.846**	0.000	0.000	0.000
SIP043	**0.496**	0.000	**0.678**	0.000	0.000	0.000
SIP001	**0.461**	0.000	**0.328**	0.000	0.000	0.000
add011	**0.473**	0.000	0.000	0.000	**0.745**	0.000
add012	**0.458**	0.000	0.000	0.000	**0.749**	0.000
add013	**0.490**	0.000	0.000	0.000	**0.596**	0.000
add014	**0.442**	0.000	0.000	0.000	**0.606**	0.000
add015	**0.499**	0.000	0.000	0.000	**0.565**	0.000
add016	**0.510**	0.000	0.000	0.000	**0.678**	0.000
add020	**0.497**	0.000	0.000	0.000	**0.543**	0.000
add021	**0.448**	0.000	0.000	0.000	**0.599**	0.000
add022	**0.468**	0.000	0.000	0.000	**0.603**	0.000
agr001	**0.611**	0.000	0.000	0.000	0.000	**0.474**
agr002	**0.635**	0.000	0.000	0.000	0.000	**0.489**

agr003	**0.651**	0.000	0.000	0.000	0.000	**0.421**
agr004	**0.550**	0.000	0.000	0.000	0.000	**0.422**
agr005	**0.523**	0.000	0.000	0.000	0.000	**0.469**
agr006	**0.620**	0.000	0.000	0.000	0.000	**0.457**
agr007	**0.621**	0.000	0.000	0.000	0.000	**0.286**
agr008	**0.621**	0.000	0.000	0.000	0.000	**0.453**
cdd001	**0.573**	0.000	0.000	0.000	**0.407**	0.000
cdd002	**0.548**	0.000	0.000	0.000	**0.219**	0.000
cdd003	**0.621**	0.000	0.000	0.000	**0.462**	0.000
cdd004	**0.468**	0.000	0.000	0.000	**0.334**	0.000
cdd005	**0.606**	0.000	0.000	0.000	**0.477**	0.000
cdd006	**0.613**	0.000	0.000	0.000	**0.384**	0.000
cdd007	**0.635**	0.000	0.000	0.000	**0.372**	0.000
cdd008	**0.637**	0.000	0.000	0.000	**0.348**	0.000
dep001	**0.760**	0.000	0.000	**0.220**	0.000	0.000
dep002	**0.724**	0.000	0.000	**0.187**	0.000	0.000
dep004	**0.791**	0.000	0.000	**0.031**	0.000	0.000
dep006	**0.775**	0.000	0.000	**0.034**	0.000	0.000
gad001	**0.506**	0.000	0.000	**0.377**	0.000	0.000
gad002	**0.554**	0.000	0.000	**0.404**	0.000	0.000
man001	**0.743**	0.000	0.000	**-0.517**	0.000	0.000
man002	**0.744**	0.000	0.000	**-0.567**	0.000	0.000
man003	**0.732**	0.000	0.000	**-0.523**	0.000	0.000
man004	**0.771**	0.000	0.000	**-0.456**	0.000	0.000
man005	**0.767**	0.000	0.000	**-0.460**	0.000	0.000
man006	**0.689**	0.000	0.000	**-0.487**	0.000	0.000
man007	**0.808**	0.000	0.000	**-0.241**	0.000	0.000
ocd001	**0.844**	0.000	0.000	**0.197**	0.000	0.000
ocd002	**0.807**	0.000	0.000	**0.125**	0.000	0.000
ocd003	**0.709**	0.000	0.000	**0.209**	0.000	0.000
ocd004	**0.826**	0.000	0.000	**0.060**	0.000	0.000
ocd005	**0.822**	0.000	0.000	**0.115**	0.000	0.000
ocd006	**0.843**	0.000	0.000	**0.107**	0.000	0.000
ocd007	**0.665**	0.000	0.000	**0.143**	0.000	0.000
ocd008	**0.766**	0.000	0.000	**0.131**	0.000	0.000
ocd011	**0.712**	0.000	0.000	**0.196**	0.000	0.000
ocd012	**0.721**	0.000	0.000	**0.134**	0.000	0.000
ocd013	**0.699**	0.000	0.000	**0.119**	0.000	0.000
ocd014	**0.763**	0.000	0.000	**0.061**	0.000	0.000
ocd015	**0.732**	0.000	0.000	**0.092**	0.000	0.000
ocd016	**0.714**	0.000	0.000	**0.150**	0.000	0.000
ocd017	**0.719**	0.000	0.000	**0.090**	0.000	0.000
ocd018	**0.629**	0.000	0.000	**0.095**	0.000	0.000
ocd019	**0.561**	0.000	0.000	**0.073**	0.000	0.000
odd001	**0.588**	0.000	0.000	0.000	**0.436**	0.000

odd002	**0.573**	0.000	0.000	0.000	**0.515**	0.000
odd003	**0.532**	0.000	0.000	0.000	**0.568**	0.000
odd005	**0.553**	0.000	0.000	0.000	**0.486**	0.000
odd006	**0.634**	0.000	0.000	0.000	**0.397**	0.000
pan001	**0.621**	0.000	0.000	**0.275**	0.000	0.000
pan003	**0.692**	0.000	0.000	**0.156**	0.000	0.000
pan004	**0.779**	0.000	0.000	**0.159**	0.000	0.000
phb001	**0.276**	0.000	0.000	0.000	0.000	**0.309**
phb002	**0.340**	0.000	0.000	0.000	0.000	**0.350**
phb003	**0.422**	0.000	0.000	0.000	0.000	**0.282**
phb004	**0.270**	0.000	0.000	0.000	0.000	**0.355**
phb005	**0.186**	0.000	0.000	0.000	0.000	**0.263**
phb006	**0.456**	0.000	0.000	0.000	0.000	**0.314**
phb007	**0.418**	0.000	0.000	0.000	0.000	**0.388**
phb008	**0.365**	0.000	0.000	0.000	0.000	**0.199**
scr001	**0.494**	0.000	0.000	0.000	**0.163**	0.000
scr006	**0.487**	0.000	0.000	0.000	**0.357**	0.000
scr007	**0.651**	0.000	0.000	**0.210**	0.000	0.000
scr008	**0.545**	0.000	0.000	0.000	**0.255**	0.000
sep500	**0.462**	0.000	0.000	0.000	0.000	**0.168**
sep508	**0.413**	0.000	0.000	0.000	0.000	**0.202**
sep509	**0.433**	0.000	0.000	0.000	0.000	**0.226**
sep510	**0.525**	0.000	0.000	**0.085**	0.000	0.000
sep511	**0.310**	0.000	0.000	0.000	0.000	**0.108**
soc001	**0.444**	0.000	0.000	0.000	0.000	**0.638**
soc002	**0.436**	0.000	0.000	0.000	0.000	**0.557**
soc003	**0.383**	0.000	0.000	0.000	0.000	**0.708**
soc004	**0.449**	0.000	0.000	0.000	0.000	**0.685**
soc005	**0.486**	0.000	0.000	0.000	0.000	**0.661**
sui001	**0.647**	0.000	0.000	**0.185**	0.000	0.000
sui002	**0.740**	0.000	0.000	**0.260**	0.000	0.000

REFERENCES:

1. Satterthwaite TD, Elliott MA, Ruparel K, Loughead J, Prabhakaran K, Calkins ME, *et al.* (2014): Neuroimaging of the Philadelphia Neurodevelopmental Cohort. *NeuroImage* 86: 544–553.
2. Merikangas KR, Calkins ME, Burstein M, He J-P, Chiavacci R, Lateef T, *et al.* (2015): Comorbidity of Physical and Mental Disorders in the Neurodevelopmental Genomics Cohort Study. 135: 14.
3. Calkins ME, Moore TM, Merikangas KR, Burstein M, Satterthwaite TD, Bilker WB, *et al.* (2014): The psychosis spectrum in a young U.S. community sample: findings from the Philadelphia Neurodevelopmental Cohort. - 13: 296–305.
4. Calkins ME, Merikangas KR, Moore TM, Burstein M, Behr MA, Satterthwaite TD, *et al.* (2015): The Philadelphia Neurodevelopmental Cohort: constructing a deep phenotyping collaborative. *J Child Psychol Psychiatr* 56: 1356–1369.
5. Shanmugan S, Wolf DH, Calkins ME, Moore TM, Ruparel K, Hopson RD, *et al.* (2016): Common and Dissociable Mechanisms of Executive System Dysfunction Across Psychiatric Disorders in Youth. *American Journal of Psychiatry* 173: 517–526.
6. Kaczkurkin AN, Moore TM, Calkins ME, Ciric R, Detre JA, Elliott MA, *et al.* (2018): Common and dissociable regional cerebral blood flow differences associate with dimensions of psychopathology across categorical diagnoses. *Molecular Psychiatry* 23: 1981–1989.
7. Kaczkurkin AN, Park SS, Sotiras A, Moore TM, Calkins ME, Cieslak M, *et al.* (2019): Evidence for Dissociable Linkage of Dimensions of Psychopathology to Brain Structure in Youths. *AJP* appi.ajp.2019.1.
8. Merikangas KR, Avenevoli S, Costello EJ, Koretz D, Kessler RC (2009): National Comorbidity Survey Replication Adolescent Supplement (NCS-A): I. Background and Measures. *Journal of the American Academy of Child & Adolescent Psychiatry* 48: 367–379.
9. Sabaroedin K, Tiego J, Parkes L, Sforazzini F, Finlay A, Johnson B, *et al.* (2019): Functional Connectivity of Corticostriatal Circuitry and Psychosis-like Experiences in the General Community. *Biological Psychiatry* 86: 16–24.

10. McGlashan TH, Miller TJ, Woods SW, Rosen JL, Hoffman RE, Davidson L (2003): *Structured Interview for Prodromal Syndromes, Version 4.0*. New Haven, CT: Prime Clinical Yale School of Medicine.
11. Muthen LK, Muther BO (1998): *Mplus User's Guide*, 7th ed. Los Angeles, CA: Muthen & Muthen.
12. Rosen AFG, Roalf DR, Ruparel K, Blake J, Seelaus K, Villa LP, *et al.* (2018): Quantitative assessment of structural image quality. *NeuroImage* 169: 407–418.
13. Schaefer A, Kong R, Gordon EM, Laumann TO, Zuo X-N, Holmes AJ, *et al.* (2018): Local-Global Parcellation of the Human Cerebral Cortex from Intrinsic Functional Connectivity MRI. *Cerebral Cortex* 28: 3095–3114.
14. Daducci A, Gerhard S, Griffa A, Lemkaddem A, Cammoun L, Gigandet X, *et al.* (2012): The Connectome Mapper: An Open-Source Processing Pipeline to Map Connectomes with MRI ((C. P. Hess, editor)). *PLoS ONE* 7: e48121.
15. Tustison NJ, Cook PA, Klein A, Song G, Das SR, Duda JT, *et al.* (2014): Large-scale evaluation of ANTs and FreeSurfer cortical thickness measurements. *NeuroImage* 99: 166–179.
16. Tustison NJ, Avants BB, Cook PA, Yuanjie Zheng, Egan A, Yushkevich PA, Gee JC (2010): N4ITK: Improved N3 Bias Correction. *IEEE Trans Med Imaging* 29: 1310–1320.
17. Avants BB, Tustison NJ, Wu J, Cook PA, Gee JC (2011): An Open Source Multivariate Framework for n-Tissue Segmentation with Evaluation on Public Data. *Neuroinform* 9: 381–400.
18. Klein A, Ghosh SS, Avants B, Yeo BTT, Fischl B, Ardekani B, *et al.* (2010): Evaluation of volume-based and surface-based brain image registration methods. *NeuroImage* 51: 214–220.
19. Avants BB, Tustison NJ, Song G, Cook PA, Klein A, Gee JC (2011): A reproducible evaluation of ANTs similarity metric performance in brain image registration. *NeuroImage* 54: 2033–2044.
20. Das SR, Avants BB, Grossman M, Gee JC (2009): Registration based cortical thickness measurement. *NeuroImage* 45: 867–879.

21. Benjamini Y, Hochberg Y (1995): Controlling the False Discovery Rate: A Practical and Powerful Approach to Multiple Testing. *Journal of the Royal Statistical Society: Series B (Methodological)* 57: 289–300.
22. Steiger JH (1980): Tests for comparing elements of a correlation matrix. *Psychological Bulletin* 87: 245–251.